UNIVERSITA' DEGLI STUDI DI CATANIA

DIPARTIMENTO DI SCIENZE BIOMEDICHE E BIOTECNOLOGICHE

DOTTORATO DI RICERCA INTERNAZIONALE
BASIC AND APPLIED BIOMEDICAL SCIENCES

TESI DI DOTTORATO

Molecular Mechanisms Involved in *Escherichia coli* K1 and *Haemophilus influenzae* Type a Blood-Brain Barrier impairment

Dott.ssa Nunzia Caporarello

COORDINATORE
Prof. Massimo Libra

TUTOR
Prof.ssa Gabriella Lupo

XXX CICLO – ANNO ACCADEMICO 2016/2017

To my niece Aurora

"Se il seme non si lascia aprire da sole, terra, acqua, accogliendo il suo destino, rimane sterile. Se invece trova la ragione per rompere il guscio, si lascia ferire ed entra nel mondo con la sua fioritura e si sperimenta come dono di colori e sapori per gli altri.
Il prezzo da pagare è un dolore, una morte "apparente", ma in realtà è "più vita"".

(Alessandro D'Avenia)

ABBREVIATIONS 5

BACKGROUND: first study 6

The Blood-Brain Barrier 6

History of the BBB 6

Physiology of the BBB 7

The Neurovascular Unit 8

Endothelial cells 9

Pericytes 10

Microglia cells 11

Astrocytes 12

Bacterial Meningitis 12

Escherichia coli K1 13

Do the PC have a role in *Escherichia coli* crossing the BBB? 13

Role of phospholipases A_2 on *E. coli* K1 invasion of the brain 14

The VEGF family 14

AIM OF THE STUDY 16

MATERIALS AND METHODS 17

Chemicals, antibodies, bacteria 17

Cell cultures 17

Construction of *in vitro* BBB model 18

Electron microscopy 18

Evaluation of the barrier integrity 18

Bacterial invasion and adhesion assays 19

Cell viability 20

Immunoblotting 20

Phospholipase A_2 assay 20

Determination of PGE2 and VEGF production 20

VEGFR-1 blockade experiments 21

Statistical analysis 21

RESULTS 22

***E. coli* K1 infection determines changes of TEER and permeability to sodium fluorescein in BBEC/BRPC co-cultures** 22

***E. coli* K1 stimulates phospholipase A_2 activities, PGE2 production and VEGF release** 23

***E. coli* adhere to BBEC and BRPC but only in BBEC the invasion occurs** 26

TEM/SEM 27

VEGFR-1 is involved in *E. coli* adhesion and invasion of BBEC 28

VEGFR-1 negatively regulates BRPC survival and its blockade protects the barrier integrity 29

Reference list, first study 36

BACKGROUND: second study 43

Role and metabolism of adenosine 43

Adenosine receptors 44

HAEMOPHILUS INFLUENZAE MENINGITIS 45

Haemophilus influenzae 45

Haemophilus influenzae, serotype b 45

Haemophilus influenzae, serotype a 45

AIM OF THE STUDY 47

MATERIAL AND METHODS 48

Cell cultures 48
Construction of *in vitro* BBB model 48
***H. influenzae* preparation and infection** 49
Electron microscopy 49
Immunoblotting 49
Fluorescence microscopy 50
Evaluation of the barrier integrity 50
Bacterial invasion assay 51
Cell viability 51
ENTPDase enzymatic activity assay 51
cAMP Detection Assay 52
Statistical analysis 52
RESULTS 53
Bacterial invasion modified cell number 53
***H. influenzae* is able to enter hBMECs** 53
***H. influenzae* reduced TEER and VE-cadherin expression in hBMEC** 54
Adenosine receptors were involved in *H. influenzae* infection 55
Ectoenzyme activity 57
Bacterial infection increased cAMP production in co-cultures 59
***H. influenzae* stimulated VEGF release** 60
CREB and Rho activation in co-cultures 62
Reference list, second study 69
ACKNOWLEDGEMENTS 73
Papers published during doctorate 74

ABBREVIATIONS

BBB, Blood-Brain Barrier;

CNS, Central Nervous System;

CSF, Cerebrospinal Fluid;

NVU, Neurovascular Unit;

AJs, Adherens Junctions;

TJs, Tight Junctions;

JAMs, Junctional Adhesion Molecules;

ZO, Zonula Occludens;

TGF- β, Transforming Growth Factor β;

E.coli, Escherichia coli K1;

EC, Endothelial cells;

PC, Pericytes;

PLA2, Phospholipase A_2;

VEGF, Vascular Endothelial Growth Factor;

VEGFR, Vascular Endothelial Growth Factor Receptor;

PG, Prostaglandin

BBEC, Bovine Brain Endothelial Cells

BRPC, Bovine, Retina Pericyte Cells

TEER, Transendothelial Electric Resistance

Hia, *Haemophilus influenzae* Type a

BACKGROUND: first study

The Blood-Brain Barrier

The Central Nervous System (CNS), brain and spinal cord, controls the body's response to different stimuli, both internal and external. The physiological functions of CNS are maintained by a fine regulation if its homeostasis thanks to the blood brain barrier (BBB), located at the level of the cerebral microvasculature. In the adult human brain, the total lenght of capillaries is about 400 miles with a surface area for exchange of 12-18 m^2 (Abbott *et al*, 2010). The BBB acts as a protective barrier against possible neurotoxic molecules, such as proteins or endogenous metabolites, xenobiotics derived from the environment or ingested with the food. At the same time, BBB selectively allows the cross of ions and nutrients from blood into the CNS by active transport.

History of the BBB

At the end of the 19^{th} century, during an experiment performed administering intravenously water soluble dyes, the German immunologist Paul Ehrilch observed that all tissue outside CNS were stained, whereas brain and cerebrospinal fluid (CSF) had no color (Ehrlich, 1885). At first, this result was related to a lack of chemical affinity for the dyes specific of the brain tissues. Meanwhile, Bield and Kraus noted that, when injected intravenously, both sodium ferro-cyanide and cholic acids had no pharmacological effects on the CNS but, when they were injected intraventricurarly, the neurological complications occurred (Ribatti *et al*, 2006) thus providing evidences of the existence of a barrier between CNS and peripheral tissues. In 1890, Max Lewandowsky introduced the term "Blood-Brain Barrier" for the first time. After a few decades, Paul Ehrlich's student Edwin Goldman performed experiments in rabbits and dogs by using trypan blue dye that later clarify Ehrlich's result. Goldman observed that, when administered intravenously, trypan blue was able to stain all tissues throughout the body, except the brain and the spinal cord. Surprisingly, injecting

trypan blue directly into the CSF, through subarachnoid space, the nervous tissue was stained while the peripheral tissues was not (Goldman, 1909). Several decades later, Friedemann performed experiments by using lipid soluble dye and observed that it was able to cross the cerebral microvasculature, staining the brain. The anatomical features of BBB was established only with the advent of electron microscopy, in 1967. By using electron-sense tracer horseradish peroxidase (HRP), Reese and Karnovsky demonstrated that endothelial cells in mouse cerebral capillaries was less permeable to HRP in comparison with endothelial cells arising from heart or skeletal muscle (Reese and Karnovsky, 1967), confirming a structural difference in the junctions between cerebral endothelial cells. Now, we know that the BBB is located in the cerebral microvasculature and that it is characterized by controlled transport across, presence of intercellular tight junctions and a lack of fenestration.

Physiology of the BBB

The BBB acts as a filter against all molecules except for small lipophilic molecules with a molecular weight of 400-600 Da (Pardridge, 2001). Nevertheless, it is possible for certain macromolecules to cross the BBB thanks to some receptor-mediated systems, for example GLUT-1 glucose transporter, transferrin receptor, L1 amino acid carrier (Abbott *et al*, 2006).

TJs of the BBB restrict paracellular diffusion of many substances from the blood while lipophilic molecules are able to enter the brain by passively diffusing across the endothelial cell membranes and could be neurotoxic. In order to avoid the crossing of lipophilic xenobiotics, the BBB expresses high levels of ATP-binding cassette (ABC) transporters to pump indesiderate molecules against their concentration gradients utilizing ATP as energy. The most important ABC transporter is P-glycoprotein (Pgp). Although Pgp is expressed both luminally and abluminally, higher levels are expressed on the luminal side (Ronaldson *et al*, 2007). Organic cations, weak organic bases with hydrophobic regions and many commonly prescribed drugs represent substrates for Pgp (Miller, 2010).

Besides the ABC transporters, there are also different enzymes highly expressed at the BBB plasma membrane that act as a metabolic barrier to detoxify endogenous and exogenous molecules. Exemples are cytochrome P450, aminopeptidases, endopeptidases and cholinesterase (Dauchy *et al*, 2008).

The Neurovascular Unit

In the brain, the microvessels are phenotypically different from those distribuited in the other districts. But how brain microvessels acquire their barrier properties? In 1980s, Stewart and Wiley performed two sets of experiments: they transplanted embryonic brain fragments into the coelomic cavity, in order to expose them to non neural vessels and fragments of the embryonic mesoderm into the brain, in order to expose them to neural vessels (Stewart and Wiley, 1981). They founded that, when vascularizing into the neural *milieu*, the abdominal vessels acquired the characteristic features of the BBB, while the brain vessels insered into the non neural *milieu* were lacking of these features, confirming that the factors present in the neural environment regulate BBB differentiation. BBB is the main component of the Neurovascular Unit (NVU), made of brain microvessels, pericytes, microglia, astrocytes endfeet and neuronal process (Figure 1, Salmeri *et al.*, 2013). All these type of cells are closely connected in order to induce and maintain the physiological function of the BBB (Abbott et al, 2010).

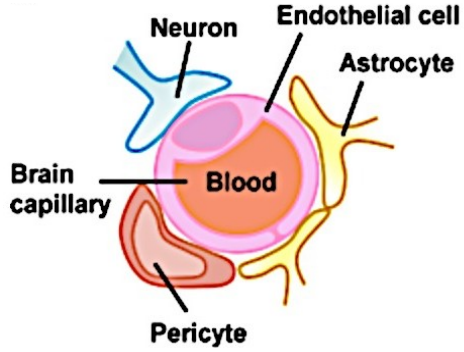

Fig. 1 - Schematic drawing of neurovascular unit

Endothelial cells

Brain endothelium is the first cell type between the blood and the brain and is responsible to bring nutrients to the brain and to avoid the cross of neurotoxic molecules. Each neuron in the human brain has its own capillary (Zlokovic, 2008). Brain endothelial cells are different from peripheric endothelial cells: in fact, they lack fenestrations, present high mitochondrial content to provide energy to support active transport, minimal pinocytotic vesicles and are characterized by the presence of tigh interendothelial junctions (Hawkins and Davis, 2005), which confer them a permeability significantly lower than that of peripheric endothelial cells (Tuma and Hubbard, 2003).

Moreover, brain vasculature is able to increase its diameter *in loco* in order to supply nutrients when neuronal metabolic demand increase, and this contractile ability is related, at least in part, to presence of pericytes, contractile cells wich also secrete various vasoactive mediators (Hamilton *et al*, 2010).

Tight interendothelial junctions are made of adherens junctions (AJ) and tight junctions (TJ) proteins. AJs proteins (such as VE-cadherin and PECAM) give the structural support to the tissue and are critical for tight junctions formation (Abbott *et al*, 2010). TJs include occludin (Hirase *et al,* 1997), claudins (Ohtsuki *et al,* 2007) and junctional adhesion molecules (JAMs) (Jia *et al*, 2013). Occludin was the first TJ protein discovered: it is a 522 amminoacids polypeptide with a molecular mass of 59.1 kDa. Occludin has N-terminal and C-terminal cytoplasmatic tails and 2 extracellular loops. N-terminal tail deletion is involved in loss of barrier property of TJs while C-terminal is important for barrier functions as well as for oligomerization of occludin (Chen *et al*, 1997) and for the interaction with regulatory proteins, such as zonula occludens 1, 2 and 3 (ZO-1, ZO-2 and ZO-3), responsible of anchoring occluding to the actin cytoskeleton (Feldman *et al*, 2005). Occludin has serin, threonine and tyrosine residues as regulatory site. An overall increase in occludin thyrosine phosphorylation lead to an increase in BBB permeability, while serine and threonine phosphorylation are associated with occludin localization within the membrane

(Takenaga *et al*, 2009). The human claudin family is made of 23 proteins with a molecular weight between 20-27 kDa and 4 transmembrane regions, 2 extracellular loops and N- and C-terminal cytoplasmic tails. Claudin-5, showing the highest expression levels of any claudin at the BBB (Lippoldt *et al*, 2000), is found in endothelial and epithelial cells of the choroid plexus.

Depending on the cell type, ZO proteins are located at TJs, adherens junctions (AJ), and/or gap junctions (Bauer *et al*, 2010). The first ZO protein discovered was ZO-1, a 220 kDa protein. (Stevenson *et al*. 1986). ZO-2, a 160 kDa protein which has a high sequence homology to ZO-1 (Gumbiner *et al*, 1991), has been less studied in BBB in comparison to ZO-1 but it is known that alterations in its expression and localization are associated with disruption of BBB (Hom *et al*, 2007). ZO-3 (130 kDa protein) is found at TJs level, but not in endothelial cells (Inoko *et al*, 2003).

Junctional adhesion molecule 1 (JAM-1) is a 40 kDa protein which contain two extracellular immunoglobulin-like (Ig-like) loops, a short cytoplasmic tail, a single transmembrane segment, and homodimerizes (Severson *et al.*, 2009).

All these proteins play a pivotal role in the restrictive BBB features.

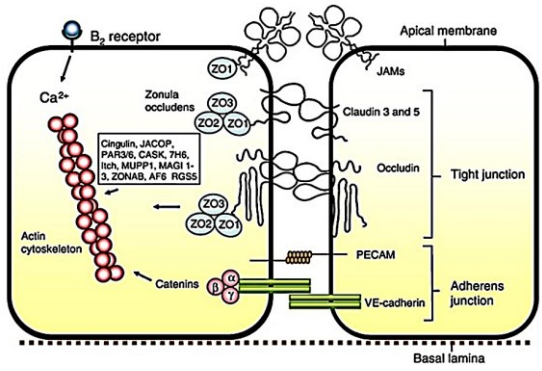

Fig. 2 - Junctional protein of the BBB (Abbott et al., 2010)!!

Pericytes

Pericytes were for the first time described by Rouget in 1879, and for this reason they were named "Rouget cells". Due to their location on the outer surface of blood capillaries and their stritct

interaction with the underlying endothelial cells, with which they share the basement membrane, in 1923 Zimmermann renamed them "Pericytes" (*peri*: around; *cyte*: cell) (Zimmermann, 1923). Pericytes cover between 22 and 37% of the cerebral capillary surface and present processes from their cell body that are in contact with more than one endothelial cell. The ratio endothelial cells/pericytes in the CNS is between 1:1 and 1:3 (Haddad-Tòvolli *et al*, 2017). Direct physical connection between pericytes and endothelial cells is provided by gap junctions, which enable the exchange of small molecules and ions. Pericytes are anchored to endothelial cells through adhesion plaques, while peg and socket contacts allow the cells to penetrate inside discontinuities in the basement membrane of vessels in contact with each other (Bergers *et al*, 2005). These junction complexes allow the transmission of mechanical contractile forces from pericytes to endothelial cells, and include cell-adhesion molecules, N-cadherin/β-catenin based adherent junctions and extracellular matrix protein, e.g. fibronectin (Gerhardt *et al*, 2003).

The role of pericytes in maintaining a proper BBB function was discovered for the first time considering the increased ratio of pericytes to endothelial cells present in the CNS in comparison to other body regions (Dìaz Flores *et al,* 2009).

Using transgenic mice PDGFRβ knockdown (in order to downregulate pericyte generation), it has been shown that pericytes are necessary for the formation of the BBB (Daneman *et al*., 2010) and that the vascular permeability is due to pericyte coverage of a capillary (Armulik *et al*, 2010).

In addition to the role on BBB development, pericytes are also involved in maintainance of the BBB during adult and age life: in fact, the number of pericytes decreases with aging while, at the same time, vascular permeability increases (Bell *et al,* 2010).

Microglia cells

Microglia are cells deputies to immune response within the CNS. In physiological conditions, microglia have small cellular bodies with long processes in direct contact with endothelial cells (Han and Suk, 2005). Under pathological conditions, microglia become activated, retract their long

processes and enlarge their cellular bodies. Once activated, microglia may secrete inflammatory cytokines and may become reactive, exhibiting phagocytic activity and acting as antigen presenting cells (Zlokovic, 2008).

Astrocytes

The most important function of perivascular astrocyte endfeet, wrapping endothelial cells, is to regulate water transport through aquaporin-4 (Tait *et al*, 2008). Astrocytes are able to induce barrier properties in endothelial cells both *in vivo* (Janzer *et al*, 1987) and *in vitro* (Rubin *et al*, 1991). Moreover, astrocytes secrete chemical mediators able to promote the BBB phenotype, such as basic fibroblast growth factor (bFGF), transforming growth factor β (TGF-β) and glial derived neurotrophic factor (GDNF). On the other hand, endothelial cells secrete mediators that promote growth and differentiation of astrocytes, thus underlying the close relation between these two type of cell (Mi *et al,* 2001).

Bacterial Meningitis

Bacterial Meningitis is a common and severe CNS infection, which is often fatal and over 50% of the survivors develop neurological complications, such as epilepsy, increased intra-cranial pressure, stroke and educational deficits in later life (Hoffman O *et al*, 2009). There are different pathogens associated with bacterial meningitis: *Streptococcus pneumoniae*, *Streptococcus agalatiae*, *Neisseria meningitidis*, *Listeria monocytogenes*, *Escherichia coli K1* and *Haemophilus influenzae type B*. The bacteria responsible of meningitis are often member of the human microbiome of gut, skin and mucous membranes of healthy humans (Cogen *et al*., 2008) which can gain virulence factors lead to penetration of epithelial and endothelial barriers and invasive disease. Before to infect CNS, bacteria must survive and persiste within the blood circulation because only the bacteria that survive in the bloodstream possess high penetration rate across the brain endothelium (Dando *et al.*,

2014). Through the years, bacterial meningitis has remained an infection with a high mortality rate, particularly in very young and elderly patients, despite advances in antimicrobial therapy (Kim, 2008). The reason for the poor outcome has been attributed to limited knowledge of pathogenesis and pathophysiology of the disease.

Escherichia coli K1

Regarding *Escherichia coli*, more than 80% of the neuropathogenic strains express the K1 capsule. This capsule is made of homopolymer of □-2,8-linked N-acetylneuraminic acid. Although most cases of *Escherichia coli* meningitis occur via haematogenous spread, microbial and host factors responsible for the ability of neurotropic strains of *Escherichia coli* to cross the BBB are still missing. After infection, release of pro-inflammatory mediators such as cytokines and prostaglandins (PGs) by leucocytes, endothelial cells, astrocytes, microglial cells and other cells in the central nervous system was stimuled, leading to an increase in the permeability of the BBB (Engblom *et al*., 2002; Zhu *et al*., 2010). *E. coli* K1 invasion of brain EC is promoted by IQGAP1 (Ras GTPase-activating-like protein) (Krishnan *et al*., 2012) and is responsible for TJs disruption.

Do the PC have a role in *Escherichia coli* crossing the BBB?

PCs are structural cells that helps to promote vascular integrity and their loss or dysfunction could play a critical role in the pathogenesis of meningitis.

PC are the cells closest brain EC, with which they share a common basement membrane, but they have not been investigated in a co-culture BBB model understanding the molecular mechanism of bacterial invasion. PC are able to secrete soluble factors, leading to the upregulation of BBB functions (Hori *et al*., 2004; Dohgu *et al*., 2005; 2011; Takata *et al*., 2007; Nakagawa *et al*., 2009). Recently, it has been reported that lipopolysaccharide-induced sepsis in mice is responsible for the detachment of brain PC from the basal lamina with disruption of the BBB (Nishioku *et al*., 2009).

Other studies have revealed that PC deficiency in the CNS leads to BBB breakdown and brain hypoperfusion resulting in secondary neurodegenerative changes (Winkler *et al*., 2011) ans that loss of pericytal function can result in development of CNS disease (Bonkowski *et al*., 2011).

Role of phospholipases A_2 on *E. coli* K1 invasion of the brain

PGs and leukotrienes (LTs) are arachidonate metabolites and contribute to *E. coli* K1 invasion of microvascular EC and crossing of BBB (Zhu *et al*, 2010). Arachidonic acid (AA) derives from phospholipids by the action of different isoforms of PLA_2s and is converted to PGs or LTs by the action of cyclooxygenase (COX) and 5-lipoxygenase, respectively. There are 3 different PLA_{2s} isoforms: cytosolic PLA_2 ($cPLA_2$), Ca^{2+}-independent intracellular PLA_2 ($iPLA_2$) and Ca^{2+}-dependent secretory PLA_2 ($sPLA_2$) that differ from each other in terms of substrate specificity, Ca^{2+} requirement, lipid modification, translocation to cellular membranes and AA release (Alberghina, 2010).

The VEGF family

The vascular endothelial growth factor (VEGF) is a critical regulator of vasculogenesis, angiogenesis, lymphangiogenesis and vascular permeability in vertebrates. The family is made of VEGFA, VEGFB, VEGFC, VEGFD, and placental growth factor (PlGF). There are 2 VEGFA isoforms: VEGF121 and VEGF165, and both are principal mediators of tumour angiogenesis. The main signaling tyrosine kinase receptor (TKR) is VEGF receptor 2 (VEGFR2; FLK, KDR in humans), followed by VEGFR1 (FLT1) and VEGFR3 (FLT3). VEGFR1 is a "decoy" receptor, being its affinity for the growth factor high, whose kinase activity is weak, preventing VEGF from binding to VEGFR-2. VEGFR3 is mostly involved in lymphangiogenesis (Ferrara *et al.*, 2005). The PlGF and VEGFB (VEGF-related molecules) bind selectively to VEGFR-1, while VEGFA binds VEGFR-1 and VEGFR-2. VEGFC and -D bind to VEGF3, and, following a proteolytic processing, activate VEGFR-2 after binding (Ferrara *et al.*, 2016).

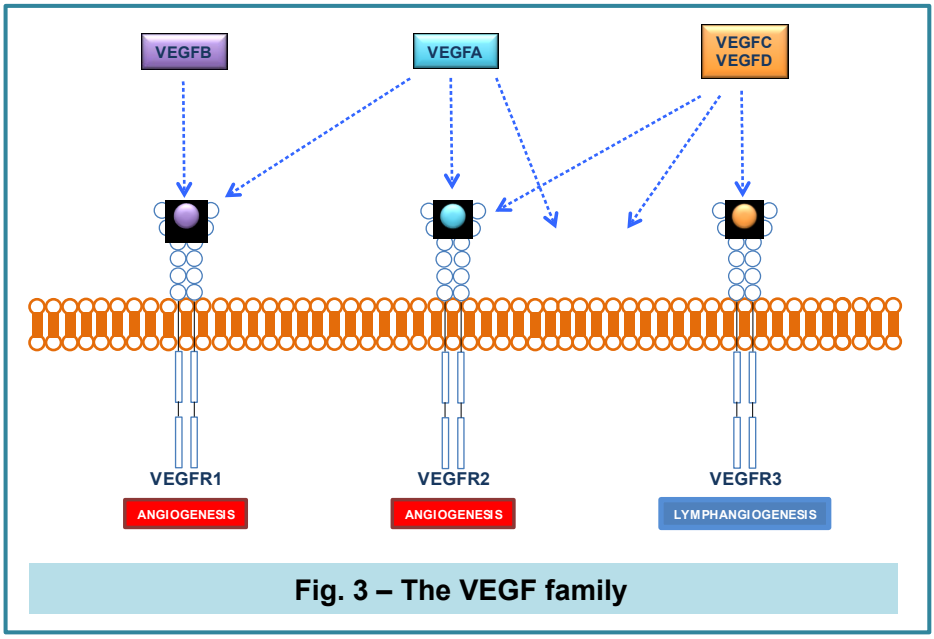

Fig. 3 – The VEGF family

VEGFR-1 is a positive regulator of angiogenesis and inflammatory responses in several human diseases such as rheumatoid arthritis (Kong *et al*., 2011), cancer (Subramanian *et al*., 2010) and bacterial meningitis. It was demonstrated that *E. coli* K1 has a critical role in the promotion of the physical association between phosphorylated VEGFR-1 and p85 subunit of PI3K, suggesting the involvement of VEGFR-1 in *E. coli* K1 invasion of microvascular ECs (Zhao *et al*., 2010).

High VEGF levels have been measured in the cerebrospinal fluid (CSF) of patients affected by bacterial meningitis with severe BBB disruption, and VEGF immunoreactivity was found in endothelium and smooth-muscle cells arising from brain specimens of patients who died of bacterial meningitis (van der Flier *et al*., 2001).

VEGF is able to stimulate PGI2 synthesis via cPLA2-mediated AA release via activation of p42/p44 MAP kinases (Wheeler-Jones *et al*., 1997). So, PKC may be a key mediator of VEGF-induced activation of the ERK pathway via increased association with Raf-1 (Gliki *et al*., 2001).

AIM OF THE STUDY

The aim of the present study was to understand how *E. coli* K1 strain is able to cross BBB. To achieve this goal, an *in vitro* model of BBB obtained by co-culturing BBEC and BRPC in transwell insert was used.

Additionally, in order to identify the contribute of PC in this process, the investigation was also extent to evaluation of the role of the pericytal VEGFR-1.

MATERIALS AND METHODS

Chemicals, antibodies, bacteria

Phospholipase A2 inhibitors, arachidonoyl trifluoromethyl ketone (AACOCF3), bromoenol lactone (BEL) and VEGF A were purchased from Calbiochem (La Jolla, CA). NS-398 (N-[2-(cyclohexyloxy)-4-nitrophenyl]-methanesulfonamide), a selective cyclooxygenase-2 inhibitor, and rabbit polyclonal against iPLA2 antibody were from Cayman Chemical (Ann Arbor, Michigan). Rabbit polyclonal against von Willebrandt factor antibody, mouse monoclonal against cPLA2, VEGFR-2, α-actin and GAPDH antibodies, rabbit polyclonal against VEGFR-1 antibody, were from Santa Cruz Biotechnology (CA). Rabbit polyclonal anti-phospho-VEGFR-2 Tyr1175 was from Cell Signaling Technologies and rabbit polyclonal anti-phospho-VEGFR-1 Tyr1333 was from Sigma Aldrich (St. Louis, MO, USA).

A rifampicin-resistant mutant of *E. coli* K1 strain (DSMZ 10723) was used for invasion of BBEC and BRPC.

Cell cultures

Primary microvascular endothelial cells from bovine brain (BBEC) were purchased from European Collection of Cell Cultures (ECACC) fed with Ham's F-10 while pure microvessel pericytes cultures were prepared from bovine retinas. After isolation, cells were cultured in DMEM with 10% fetal bovine serum, 100 U/ml penicillin and 100 μg/ml streptomycin. Morphological changes and cell viability was determined by MTT test. Pericytes were characterized by their large size and branched morphology, positive immunostaining for a-smooth muscle actin, NG2 chondrotitin sulfate proteoglycan and absence of von Willebrand factor and glial fibrillary acidic protein (GFAP) staining.

Construction of *in vitro* BBB model

Transwell inserts (Transwells, Corning, Corning, NY) were coated on the upper and bottom side with 2 mg/ml solution of rat tail collagen before being placed in complete medium (half and half DMEM/HAM's). To construct an *in vitro* model of BBB, BRPC (2×10^4 cells cm^2) were first plated on the outside of the Transwell inserts membrane and placed upside down in the well culture plate to allow adhesion. After adhesion, the Transwells were inverted and BBEC (2×10^4 cells cm^2) were seeded on the top surface of the insert (Fig. 5). Under these conditions, the two type of cells on direct contact established an *in vitro* BBB model within 3 days.

Electron microscopy

For Scanning Electron Microscopy (SEM) preparations, cells grown in co-colture on filters were fixed with 1.5% glutaraldehyde overnight, following by an additional fix in 1% OsO4 (1 h). Then, cells on the membrane were dehydrated in graded ethanol, critical point dried, sputtered with 5 nm gold layer using an Emscope SM 300 (Emscope Laboratories, Ashford, UK) and observed using a Hitachi S-4000 (Hitachi High-Technologies America, Schaumburg, IL) field emission scanning electron microscope.

For Transmission Electron Microscopy (TEM), after dehydrating in a graded series of acetone, cells were embedded in Durcupan ACM (Fluka Chemika-Biochemika, Buchs, Switzerland). Ultrathin sections were cut using a Reichert Ultracut E microtome and double stained with uranyl acetate and lead citrate. Observations were carried out using a Hitachi H-7000 transmission electron microscope (Hitachi High-Technologies Europe GmbH, Krefeld, Germany).

Evaluation of the barrier integrity

TEER was measured using a Millicell-ERS (Millipore). Background resistance was measured using

collagen-treated Transwell inserts without cells. Values were expressed as ω x cm^2 and were calculated using the formula: (the average resistance of experimental wells – the average resistance of blank wells)*0.33 (the area of the transwell membrane).

For the determination of the flux of sodium fluorescein (Na-F) across endothelial monolayer, inserts containing cells were transferred to 12- well plates containing 1.5 ml of Ringer-Hepes buffer (136 mM NaCl, 0.9 mM $CaCl_2$, 0.5 mM $MgCl_2$, 2.7 mM KCl, 1.5 mM KH_2PO_4, 10 mM NaH_2PO_4, 25 mM glucose and 10 mM Hepes, pH 7.4) in the lower compartments (abluminal). In the inserts (luminal compartment), culture medium was replaced by 0.5 ml of buffer containing 10 μg ml^{-1} Na-F. The inserts were transferred at 5, 15 and 30 min to a new well containing Ringer-Hepes buffer. The concentrations of the marker molecule in samples were determined by fluorescence multiwell plate reader (PerkinElmer; excitation wavelenght: 485 nm, emission wavelenght: 535 nm). Transendothelial permeability coefficient (Pe) was calculated measuring flux across cell-free inserts.

Bacterial invasion and adhesion assays

Bacteria (10^7 cfu per well) were added to confluent cells in mono-culture or in co-culture on Transwell inserts (37°C, 60 min). The number of intracellular bacteria was determined after incubation with gentamicin (100 μg/ml) for 1 h at 37°C to kill extracellular bacteria. Cells were washed and lysed with 0.5% Triton X-100. The released intracellular bacteria were evaluated by seeding on LB agar plates and counting the number of colonies the day after. In duplicate experiments, the total cell-associated bacteria were determined as described for invasion, except that the gentamicin step was omitted (in order to include extracellular, adherent to membrane bacteria). Results were expressed as per cent invasion [100 × (number of intracellular bacteria recovered)/(number of bacteria inoculated)].

Cell viability

After incubation of BBEC/BRPC in co-culture with *E. coli* K1 (60 min), cells from inserts were trypsinized separately, cell suspensions were mixed with a 0.4% (w/v) trypan blue solution, and the number of live cells was determined using a haemocytometer. Cells failing to exclude the dye were considered non-viable. Each infection was performed in triplicate and counted four times each.

Immunoblotting

The lysates of BBEC incubated with *E. coli* strains for 60 min were prepared for Western blotting (Giurdanella *et al*., 2011). Membranes were incubated overnight at 4°C with primary antibodies against cPLA2, iPLA2, VEGFR-1, VEGFR-2, phospho-VEGFR-2 Tyr1175 or phospho-VEGFR-1 Tyr1333 (dilution, 1:1000) and then incubated with secondary antibodies (dilution, 1200) for 1 h at room temperature.

Phospholipase A_2 assay

BBEC and BRPC in mono- or in co-culture were pre-incubated for 60 min in culture medium in the absence or presence of either 50 μM $AACOCF_3$ or 2.5 μM BEL. The cells were then refed with fresh culture medium containing the inhibitors in presence or in absence of *E. coli* K1 for 60 min. Controls were performed by incubation of co-cultures with inhibitors for 120 min in absence of bacteria. After incubations, cells grown on both sides of the inserts were scraped separately, lysed (Anfuso *et al*., 2007) and equal amounts of cell lysates were incubated in a 96-well plate with the substrate arachidonoyl-thio-phosphatidylcholine (ATPC), using $cPLA_2$ assay kit (Cayman Chemicals, Ann Arbor, MI, USA) according to manufacturer's instructions.

Determination of PGE2 and VEGF production

BBEC and BRPC in mono- or in co-culture were pre-incubated for 60 min in the absence or

presence of 50 μM $AACOCF_3$ or 2.5 μM BEL or 5 μM NS-398. The cells were then refed with fresh culture medium containing the inhibitors in presence or in absence of *E. coli* K1 for 60 min. Supernatants were collected and used for PGE_2 determination (Cayman Chemicals, Ann Arbor, MI, USA). Conditioned medium was removed from mono- and co-cultures and analysed for VEGF by ELISA (R&D Systems, Minneapolis, MN, USA), as specified by the manufacturer's instructions.

VEGFR-1 blockade experiments

For BBEC/BRPC simultaneous blockade experiments, co-culture were treated with VEGFR-1 Ab (2 μg ml^{-1}) for 60 min before treatment with *E. coli* K1 for 60 min. Parallel co-cultures without VEGFR-1 blockade were performed.

For BBEC (but not BRPC) VEGFR-1 blockade experiments, BBEC were grown on the top surface of the Transwell insert and incubated with VEGR-1 Ab. Then, inserts were inverted and BRPC were seeded on the outside of the insert. After BRPC adhered, the inserts were reinserted into six-well plates and the *in vitro* BBB model, in which BBEC were blocked by VEGFR-1 Ab, was established within 3 days.

For BRPC (but not BBEC) VEGFR-1 blockade experiments, BRPC were first plated on the outside of the Transwell inserts. After adhesion of BRPC, the inserts were reinserted into six-well and cells were incubated with VEGFR-1 Ab. Then, BBEC were seeded on the top surface of the insert and the *in vitro* BBB model, in which BRPC were blocked by VEGFR-1 Ab, was established within 3 days.

Statistical analysis

Statistical significance between two groups was analysed by Student's test. One-way analysis of variance (anova), followed by Tukey's *post hoc* test, was used to compare the means for the multiple groups. The P-value < 0.05 was considered statistically significant.

RESULTS

***E. coli* K1 infection determines changes of TEER and permeability to sodium fluorescein in BBEC/BRPC co-cultures**

TEM of BBEC growing on Transwell filter in the *in vitro* BBB model is shown in Fig. 4. TJ sealing adjoining BBEC are evident.

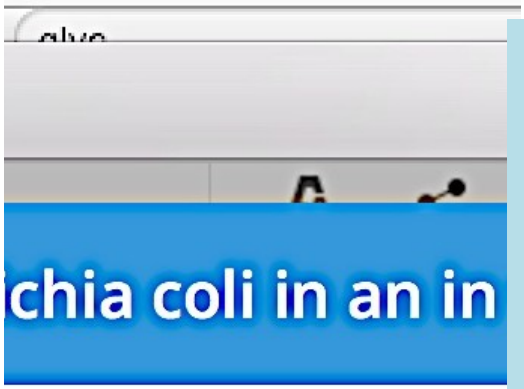

Fig. 4 – TJs in BBEC
Transmission electron micrographs of bovine brain microvascular endothelial cells (BBEC). Two elongated primary BBEC cultured onto the Transwell membranes display typical morphology of the endothelial cells. The black arrows indicate the tight junctional elements between two primary BBEC.
Bar equals to 200 nm.

The BBB model was validated by measuring TEER and sodium fluorescein flux across BBEC in monolayer and in co-culture with BRPC (Table 1). Co-culture showed high values of TEER and very low permeability to sodium fluorescein compared with BBEC mono-culture. Incubation for 60 min with *E. coli* K1 (10^7 cfu per well) caused a significant TEER reduction (about 3.2-fold) and an increase in permeability (about 2.3-fold) in comparison to BBEC/BRPC control co-cultures.

		TEER (ω x cm^2)	Pe (10^{-6} cm/s)
mono-culture	BBEC	85 ± 21.4	8.1 ± 0.6
mono-culture	BBEC + E. coli	60 ± 16.6	6.6 ± 0.8
co-culture	BBEC/BRPC	250 ± 51.1†	3.2 ± 0.15†

Table 1 – Evaluation of the barrier integrity
Evaluation of the barrier integrity. TEER and permeability to sodium fluorescein (Pe) determination in microvascular endothelial cells in mono- and in co-culture, in the absence or presence of *E. coli* K1 strain. BBEC (40,000 cells/cm^2) were cultured in monolayers in Ham's F-10 medium containing 10% FBS or were grown on the top surface of the Transwell insert (6-well type, 3.0-mm pore size) in which BRPC (40,000 cells/cm^2) were first plated on the outside of the membrane, in 50% DMEM plus 50% F-10 HAM's containing 10% FBS. After 3 days, the cells were incubated in the absence or presence of *E. coli* (10^7 CFU/well) for 60 min and measurements of TEER and cell permeability on BBEC were performed. Values were expressed as ω x cm^2 and were calculated by the formula: [the average resistance of experimental wells - the average resistance of blank cells] × 0.33 (the area of the transwell membrane).
For sodium fluorescein determination, flux across cell-free inserts was measured and transendothelial permeability coefficient (Pe) was calculated. Values (means ± SEM) are from three independent experiments (n=3). Statistically significant differences of TEER and Pe, measured in BBEC in co-culture as compared to mono-culture are indicated by † (†$p < 0.01$) and values from *E. coli*-stimulated BBEC as compared to control non-stimulated BBEC are indicated by asterisks (**$p < 0.01$).

***E. coli* K1 stimulates phospholipase A_2 activities, PGE2 production and VEGF release**

BBEC in mono- and co-culture stimulated with *E. coli* K1, showed a strong PLA2 activity (about 2.2-fold in mono- and 2.6-fold in co-cultures) compared with the unstimulated BBEC, whereas in BRPC it was weakly stimulated. The presence of 50 µM AACOCF3 (PLA_2 activity dual blocker) or 2.5 µM BEL (iPLA2 inhibitor) for 120 min (pre-incubation of 60 min followed by incubation for 60 min in the presence of bacteria) in control BBEC mono-cultures, reduced enzyme activity of 28% and 19%, respectively; in *E. coli* K1 treated BBEC mono-cultures, AACOCF3 and BEL reduced PLA_2 activity by 62% and 55%, respectively. In control BRPC mono-cultures, AACOCF3 and BEL caused a decrease by 32% and 24% respectively, and in *E. coli* stimulated BRPC mono-cultures, the inhibitors reduced PLA_2 activity by 36% and 28% respectively.

	PLA_2 activity (pmol min-1 mg-1)	Control cells	Cells + E. coli
	BBEC	19.9 ± 1.5	44.7 ± 3.2*
	BBEC + AACOCF3	14.4 ± 1.1†	17.1 ± 1.5†
	BBEC+BEL	16.1 ± 1.3	20.0 ± 1.7†
mono-culture	BRPC	13.5 ± 1.1	17.1 ± 1.3
	BRPC + AACOCF3	9.2 ± 0.8†	11.0 ± 1.2†
	BRPC + BEL	10.3 ± 1.2†	12.3 ± 0.9†
	BBEC	27.4 ± 2.5	71.2 ± 6.2*
	BBEC + AACOCF3	19.8 ± 1.3†	23.1 ± 2.1†
co-culture	BBEC+BEL	22.1 ± 2.2†	31.2 ± 2.4†
	BRPC	12.2 ± 1.1	16.1 ± 1.3
	BRPC + AACOCF3	7.7 ± 0.9	10.3 ± 0.9†
	BRPC + BEL	8.0 ± 1.2	10.2 ± 1.3†

Table 2 – PLA2 activity in BBEC and BRPC in mono- and co-culture stimulated and not-stimulated by E. coli K1
BBEC were cultured in monolayers or on the top Transwell insert in which BRPC were first plated on the outside of the membrane. All incubations were performed at 37°C in absence or presence of *E. coli* (10^7 cfu per well) for 60 min with or without 50 mM AACOCF3 or 2.5 mM BEL. Values (means SEM) are from three independent experiments (n = 3). ANOVA and the Tukey post-test were used to compare enzyme activities measurements in the 24 different experimental conditions (P < 0.05). Enzyme activities measured in *E. coli*-stimulated BBEC in comparison with control un-stimulated BBEC, are indicated by asterisk (*), and in presence of inhibitors in comparison with the values in absence of inhibitors are indicates by dagger (†).

In control BBEC/BRPC co-culture, $AACOCF_3$ and BEL reduced PLA_2 enzymatic activity by 28% and 20%, respectively. After *E. coli* K1 treatment in presence of the inhibitors, the reduction was stronger (68% and 56%, respectively). Moreover, the two inhibitors decreased PLA_2 activity in control and in *E. coli* treated BRPC by about 36%. The incubation with BEL allowed us to discriminate between the $cPLA_2$ and $iPLA_2$ activity contribution.

PGE_2 in supernatants of BBEC or BRPC in mono- and in co-culture were measured. Table 3 shows an increase in BBEC monocoltures infected with *E. coli* K1 (2.5 fold) compared with the respective control whereas bacterial incubation in presence of AACOCF3 or BEL decreased PGE2 production by 63% and 60%, respectively. The contribution in PGE2 production from *E. coli*-treated BRPC monocultures was negligible.

	PGE_2 ($pg\ ml^{-1}$)	Control cells	Cells + E. coli
	BBEC	88 ± 7.8	220 ± 21.1*
	BBEC + AACOCF3	73 ± 6.1[a]	82 ± 7.9[a]
	BBEC+BEL	78 ± 6.8[a]	88 ± 8.1[a]
mono-culture	BRPC	70 ± 6.9	73 ± 6.9[b]
	BRPC + AACOCF3	52 ± 4.8[a]	56 ± 5.1[a]
	BRPC + BEL	57 ± 5.1[a]	59 ± 5.4[a]
co-culture	BBEC/BRPC	203 ± 19.9[c]	612 ± 46.8[c*]
	BBEC/BRPC + AACOCF3	162 ± 15.8[a]	182 ± 18.8[a]
	BBEC/BRPC + AACOCF3	171 ± 16.5[a]	192 ± 21.1[a]

Table 3 - Prostaglandin (PGE2) production in BBEC and BRPC in mono- and co-culture stimulated and non-stimulated by *E. coli* K1
a. The statistically significant differences in PGE2 production of cultures incubated with PLA2 inhibitors in comparison with the respective in absence of inhibitors.
b. The statistically significant differences in PGE2 release in untreated BRPC mono-cultures in comparison with untreated BBEC mono-cultures.
c. The statistically significant differences, between not- and stimulated co-cultures versus the respective mono-cultures.
BBEC were cultured in monolayers or on the top surface of the Transwell insert in which BRPC were first plated on the outside of the polycarbonate membrane. Cell culture supernatants from mono- and co-cultures in absence (control) and presence of *E. coli*, with or w/o 50 mM AACOCF3 or 2.5 mM BEL, were assayed for PGE2 production. Inhibitors were added to the culture medium 60 min before E. coli addition. Values (means SEM) are from three independent experiments (n = 3). ANOVA and the Tukey post-test were used to compare PGE2 production in the 18 different experimental conditions ($P < 0.05$). Stimulated cells versus control cultures (not stimulated by bacteria), are indicated by asterisk (*).

E. coli K1 treatment of BBEC/CRPC co-cultures increased PGE2 production by 3.0 fold in comparison with the respective untreated co-cultures. Furthermore, in the supernatants of *E. coli*-stimulated co-cultures, incubated in presence of PLA_2 inhibitors $AACOCF_3$ or BEL, PGE_2 levels decreased by about 70% and 68%, respectively.

BBEC monocultures produced low amounts of VEGF in the conditioned medium. Incubation of BBEC monocoltures with *E. coli* K1 led to a 3.1 fold increase in the release of VEGF (Table 4). Conversely, untreated BRPC monocultures expressed VEGF at basal levels 1.6-fold higher than untreated BBEC monocultures and the presence of *E. coli* did not changed the secretion. *E. coli* treatment of co-cultures induced an 3.2 fold increase in comparison with control untreated co-cultures. Incubation of *E. coli*-treated BBEC monocultures with AACOCF3, BEL or with COX-2-specific inhibitor NS-398 reduced *E. coli*-induced VEGF release by 70%, 67% and 71% respectively. Incubation of untreated co-cultures with the three inhibitors reduced VEGF release by

about 33%, while in *E. coli*-treated co-cultures AACOCF3, BEL and NS-398 reduced VEGF release by 77%, 75% and 79%, respectively. The effect of the inhibitors on VEGF release in untreated and *E. coli*-treated BRPC monocultures was about 22% and 21% respectively.

	VEGFA (pg ml^{-1})	Control cells	Cells + E. coli
mono-culture	BBEC	22.3 ± 1.9	70.4 ± 7.5*
	BBEC + AACOCF3	13.5 ± 1.4^{a}	21.1 ± 2.3a
	BBEC+BEL	16.3 ± 1.8^{a}	23.2 ± 3.4a
	BBEC + NS-398	15.5 ± 1.7^{a}	20.4 ± 2.3a
	BRPC	35.7 ± 3.2^{b}	33.8 ± 2.9b
	BRPC + AACOCF3	27.3 ± 2.3^{a}	26.1 ± 2.5a
	BRPC + BEL	29.0 ± 3.1^{a}	27.2 ± 3.1a
	BRPC + NS-398	26.8 ± 2.3^{a}	26.8 ± 3.2
co-culture	BBEC/BRPC	80.7 ± 6.7^{c}	260.5 ± 22.1*
	BBEC/BRPC + AACOCF3	54.2 ± 4.7^{a}	60.4 ± 5.3^{a}
	BBEC/BRPC + BEL	56.4 ± 4.2^{a}	65.1 ± 5.6^{a}
	BBEC/BRPC + NS-398	50.8 ± 4.3^{a}	55.2 ± 4.7^{a}

Table 4 - VEGFA determination in BBEC and BRPC in mono- and co-culture stimulated and non-stimulated by E. coli K1
a. Statistically significant differences in VEGF release of cultures incubated with inhibitors in comparison with the respective in absence of inhibitors. **b.** The statistically significant differences in VEGF release in untreated BRPC mono-cultures in comparison with untreated BBEC mono-cultures. **c.** The statistically significant differences in VEGF release in co-cultures in comparison with the mono-cultures. BBEC and BRPC were cultured in monolayers or on Transwell. Aliquots of medium from mono- and co-cultures in absence and in presence of *E. coli* were incubated with bovine VEGF-A antibody. Values (means SEM) are from three independent experiments (n = 3). ANOVA and the Tukey post-test were used to compare VEGF release in the 24 different experimental conditions (P < 0.05). Statistically significant differences of *E. coli*-stimulated mono- and co-cultures in comparison with not stimulated (cultures are indicated by asterisk (*).

E. coli adhere to BBEC and BRPC but only in BBEC the invasion occurs

SEM images of BBEC, (Fig. 5, A and B) or BRPC (Fig. 5, C and D), after incubation with *E. coli* K1, show the cells with an elongated and spindle phenotype, with numerous microvilli distributed on most of the cell surface (Fig. 5 A). The images at higher magnification show the bacteria attached to the apical surface of the BBEC in contact with microvilli (Fig. 5 B).

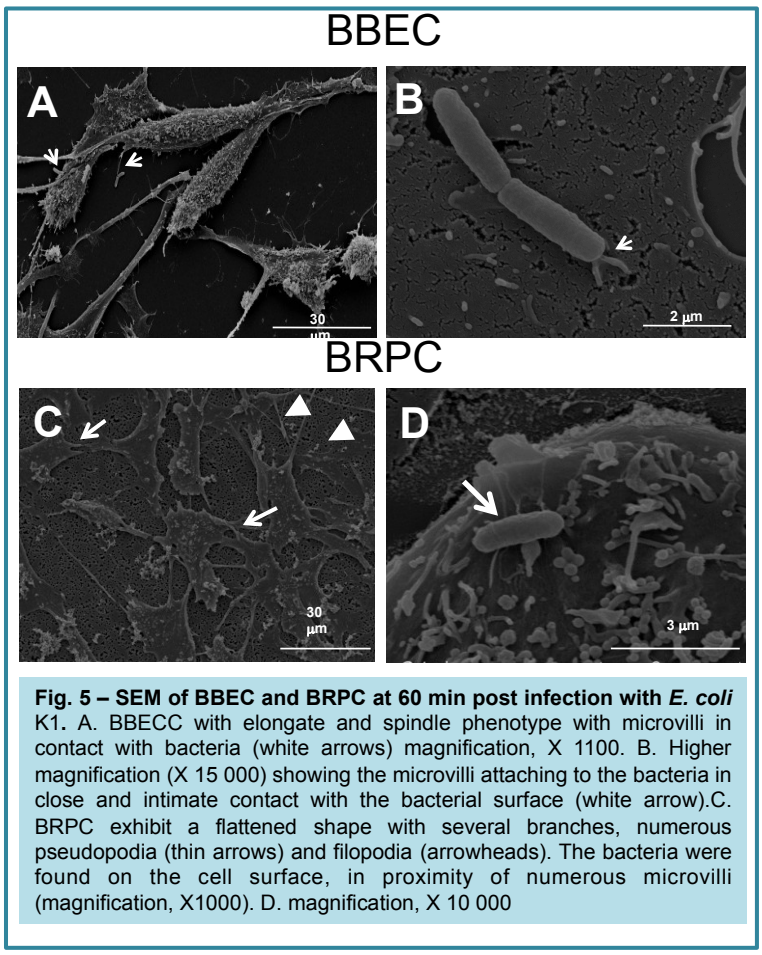

Fig. 5 – SEM of BBEC and BRPC at 60 min post infection with *E. coli* K1**.** A. BBECC with elongate and spindle phenotype with microvilli in contact with bacteria (white arrows) magnification, X 1100. B. Higher magnification (X 15 000) showing the microvilli attaching to the bacteria in close and intimate contact with the bacterial surface (white arrow).C. BRPC exhibit a flattened shape with several branches, numerous pseudopodia (thin arrows) and filopodia (arrowheads). The bacteria were found on the cell surface, in proximity of numerous microvilli (magnification, X1000). D. magnification, X 10 000

BRPC are branched and flat with short microvilli on the surface area (Fig. 5C). Few bacteria were found attached to the smooth part of the BRPC surface without any sign of specific membrane interaction (Fig. 5 D).

TEM/SEM

Figure 6 A shows BRPC with numerous bacteria on the cell surface where they remain and no endocytosed bacteria were found. In *E. coli*–BBEC interaction, electron-dense bacteria both intra- and extracellular were seen and also BBEC formed microvilli-like protrusions that surrounded and endocytosed the bacteria (Fig. 6 B).

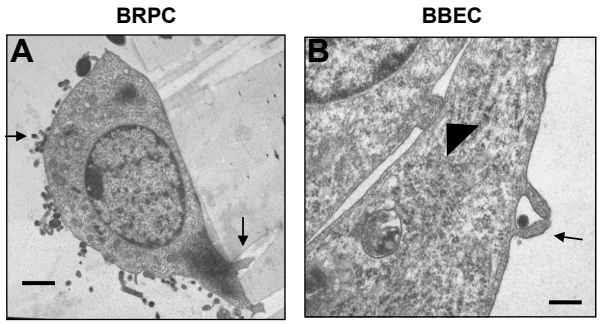

Fig. 6. Transmission electron micrographs of BRPC (A) and BBEC (B–D) infected with *E. coli* K1for 60 min
A. BRPC on Transwell showing cellular protrusions infiltrating the filter pores (black arrow). Bacteria are present on the surface (dark black) but not inside the cells (bar = 1 μm). B. Electron-dense (dark black) bacteria were seen extracellularly and some bacteria were intracellularly engulfed inside membranes-bound vacuoles (thick black arrows) (bar = 1.25 μm).

VEGFR-1 is involved in *E. coli* adhesion and invasion of BBEC

Western blot analysis showed that VEGFR-1 expression in BRPC mono- and co-cultures was 2.0 fold and 2.2 fold higher than that of BBEC in mono- and in co-cultures, respectively (Fig. 7 A). VEGFR-2 expression did not change in BBEC grown in contact with BRPC in respect to BBEC monoculture. Interestingly, VEGFR-2 protein was not detected in BRPC (Fig. 7 B).

In order to understand the involvement of VEGF receptors in *E. coli* K1 adhesion and invasion, assays were performed in presence of VEGFR-1 or VEGFR-2 antibodies (Ab). Fig. 7 C show that VEGFR-1 Ab and VEGFR-2 Ab have no effect on *E. coli* adhesion to BBEC both in mono- and in co-cultures, as well as on *E. coli* adhesion after addition to BRPC in mono- and in co-cultures (Fig. 7 D). VEGFR-1 Ab significantly reduced *E. coli* invasion in BBEC by 30% and by 48% in mono- and in co-cultures, respectively (Fig. 7 E), while VEGFR-2 did not cause any change in the *E. coli* invasion of BBEC. These results indicate a positive correlation between the block of VEGFR-1 and the block of *E. coli* K1. Treatment of BBEC with 10 ng/ml VEGF for 15 and 30 min in absence or in presence of VEGFR-2 Ab showed an increase of phosphorylation of VEGFR-2 at Tyr1175, as assessed by Western blot, while treatment with 10 ng/ml of VEGF in presence of 2 μg/ml VEGFR-2 antibody inhibited VEGFR-2 phosphorylation (Fig. 7 F). Experiments were also performed by treating BBEC with 10 ng/ml^{-1} VEGF for 15 and 30 min in absence or in presence of

VEGFR-1 Ab. Phosphorylation of VEGFR-1 at Tyr1333 was observed in BBEC treated for 15 and 30 min with VEGF.

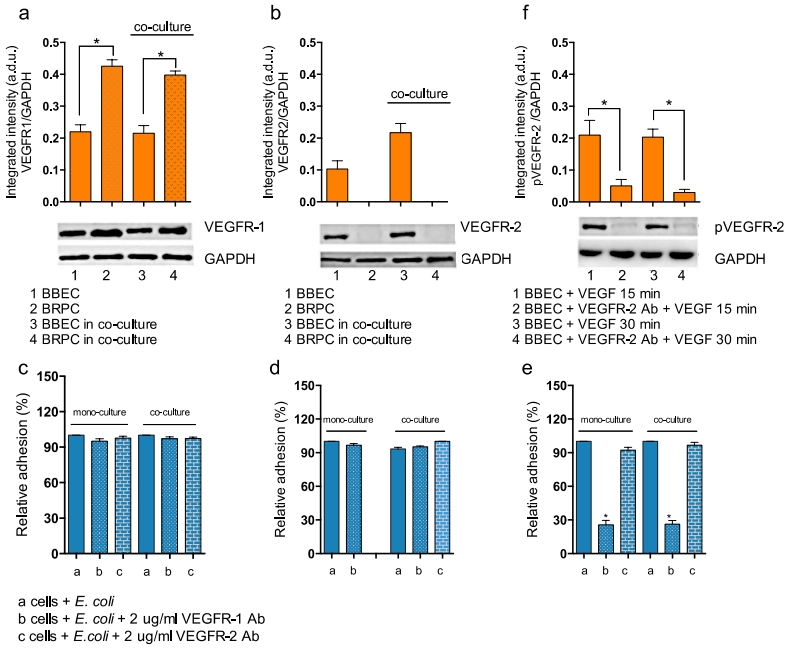

Fig. 7 - Expression of VEGFR1/2, evaluated by Western blot analyses, and *E. coli* K1 adhesion and invasion of BBEC and BRPC in mono- and in co-culture

VEGFR-1 (A) and VEGFR-2 (B) protein expression in BBEC and BRPC incubated *with E. coli* K1 (60 min). Representative gel analyses are shown; values represent means ± SD from three separate experiments. Statistically significant differences by pairwise Student's *t*-test are indicated by asterisks ($P < 0.05$). *E. coli* K1 adhesion on mono- and co-culture BBEC (C) and BRPC (D) and invasion on mono- and co-culture BBEC (E), in absence or in presence of 2 µg/ml anti-VEGFR-1 or 2 µg/ml anti-VEGFR-2 antibodies, are expressed as relative percent. Expression of phospho-VEGFR-2 Tyr1175 was evaluated by Western blot analyses after treatment of BBEC with 10 ng/ml VEGF for 15 and 30 min in absence or in presence of VEGFR-2 Ab, to have the evidence that the anti-VEGFR-2 antibody was effective in the binding to its own receptor (F). Values are means ± SD of three independent experiments ($n = 3$). Statistically significant differences are indicated by asterisk for the comparison between the invasion of BBEC mono- or co-culture infected by *E. coli* in presence of VEGFR-1 Ab versus the invasion of the respective mono- or co-cultures infected in absence of VEGFR-1 Ab ($P < 0.05$).

VEGFR-1 negatively regulates BRPC survival and its blockade protects the barrier integrity

To clarify if the prevention of the pericyte death and monolayer permeability can be attributed to VEGFR-1, experiments blocking the receptor by its specific antibody were performed on co-cultures or single cell type monocultures. After incubation of BBEC/BRPC co-cultures with *E. coli* K1, TEER decreased by 64% and permeability to sodium fluorescein increased by 3.2 fold in comparison with non-infected co-cultures (Fig. 8 C and D).

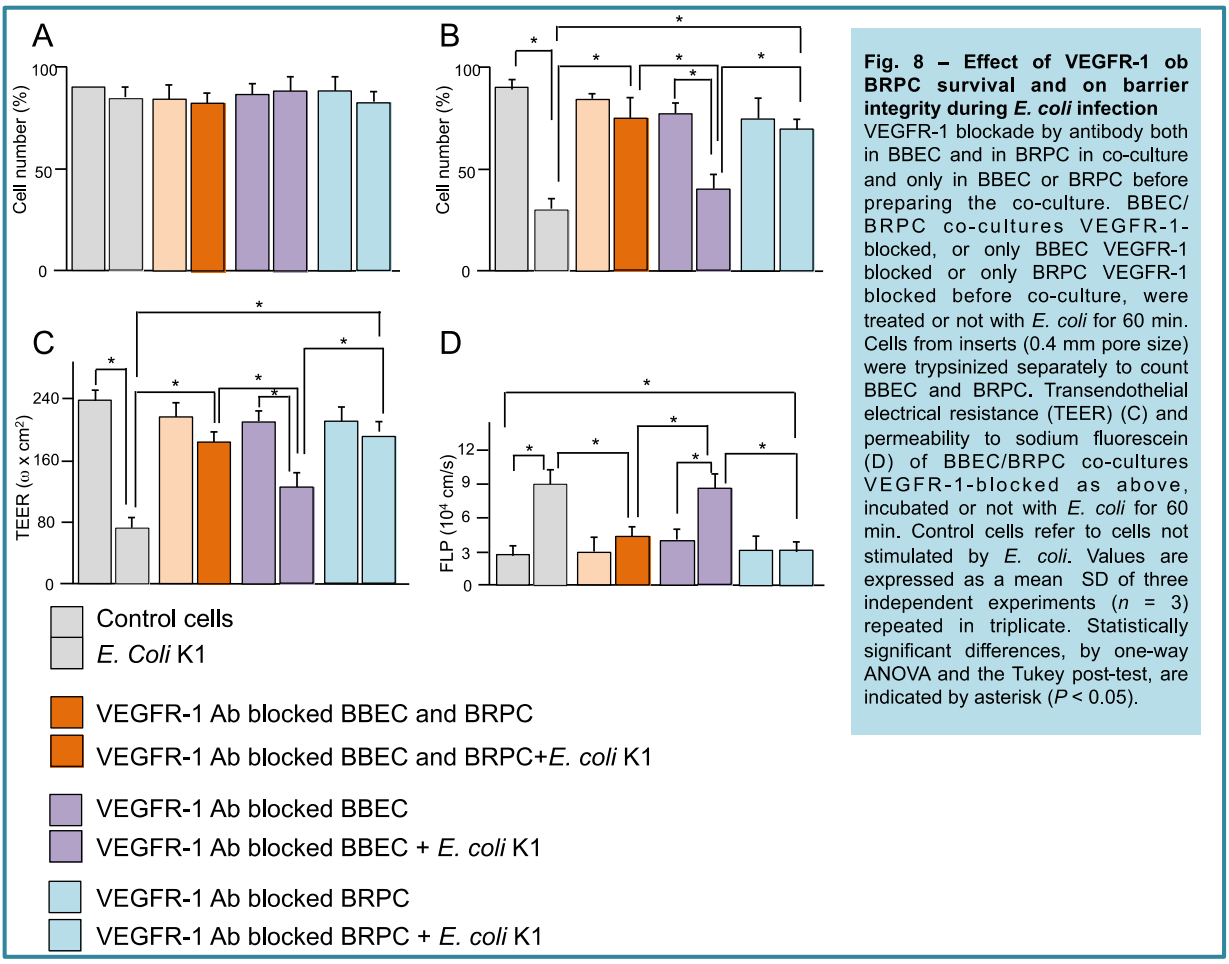

Fig. 8 – Effect of VEGFR-1 ob BRPC survival and on barrier integrity during *E. coli* infection
VEGFR-1 blockade by antibody both in BBEC and in BRPC in co-culture and only in BBEC or BRPC before preparing the co-culture. BBEC/BRPC co-cultures VEGFR-1-blocked, or only BBEC VEGFR-1 blocked or only BRPC VEGFR-1 blocked before co-culture, were treated or not with *E. coli* for 60 min. Cells from inserts (0.4 mm pore size) were trypsinized separately to count BBEC and BRPC. Transendothelial electrical resistance (TEER) (C) and permeability to sodium fluorescein (D) of BBEC/BRPC co-cultures VEGFR-1-blocked as above, incubated or not with *E. coli* for 60 min. Control cells refer to cells not stimulated by *E. coli*. Values are expressed as a mean SD of three independent experiments (n = 3) repeated in triplicate. Statistically significant differences, by one-way ANOVA and the Tukey post-test, are indicated by asterisk ($P < 0.05$).

In co-culture, simultaneous block of VEGFR-1 in presence of *E. coli* K1 was able to preserve BRPC viability by almost 3 fold in comparison with infection in the absence of VEGFR-1 Ab (Fig. 8 B). Moreover, in presence of *E. coli* K1 and receptor blockade, TEER values increased by 2.3 fold and permeability decreased by 2.2 fold in comparison with infected co-cultures in absence of receptor blockade. Furthermore, only 10% of TEER reduction and a 20% of increase in permeability were found in comparison with non-infected control cells in co-culture (Fig. 8 C and D).

When only the BBEC were treated with VEGFR-1 Ab and *E. coli* K1, 45% of BRPC adhering to the co-culture insert was found (Fig. 8 B), while BBEC number was unchanged (Fig. 8 A). Moreover, a significant decrease in TEER values (about 56%) and a significant increase in permeability (approximately 2.8 fold) in *E. coli* infected in comparison with non-infected co-cultures were found. Furthermore, a 38% of TEER decrease and a 2 fold permeability increase were

found in comparison with *E. coli* K1 infected co-cultures in which both BBEC and BRPC were blocked by VEGFR-1 Ab (Fig. 8 C and D). These results demonstrated that VEGFR-1 Ab was able to partially reduce *E. coli* K1 internalization (about 50%, as shown in Fig. 7) but not to completely avoid the activation of signalling pathway leading to VEGF release, detachment of BRPC and loss of barrier properties.

Blockade of only BRPC in presence of *E. coli* K1 did not change BRPC number in co-culture (Fig. 8 B), whose value was very similar to that of BRPC in absence of infection. Moreover, the values of TEER and permeability in this experimental condition were similar to non-infected control cells in co-culture. Furthermore, TEER increased by 1.7 fold and by 2.4 fold and permeability decreased by 60% and 64% in comparison with *E. coli* K1 infected co-cultures in which only BBEC were blocked by VEGFR-1 Ab and in comparison with *E. coli* infected co-cultures in which no blocking was induced, respectively (Fig. 8 C and D). Probably, in absence of VEGFR-1 Ab on BBEC, *E. coli* K1 is able to invade BBEC without limits and to activate the signalling pathway leading to VEGF production in large amounts. The VEGF released by BBEC cannot bind VEGFR-1 on BRPC, because blocked by the specific antibody, it therefore does not result in the detachment of pericytes. In this experimental condition, about 90% of BRPC adhered to co-culture and the values of TEER and permeability were very similar to those of the non-infected co-cultures.

These results demonstrate that the prevention of pericyte loss and monolayer permeability can be attributed to VEGF blockade.

To further confirm our results, experiments on BBEC/BRPC co-cultures incubated with *E. coli* K1 for 30, 60, 90 and 120 min, in absence or in presence of VEGFR-1 or VEGFR-2 Abs were performed.

As shown in Fig. 9, TEER values gradually decreased after 30 min *E. coli* K1 treatment (37% reduction) to reach 60% following incubation for 60 and 120 min (panels A, B and C). The presence of VEGFR-1 Ab, but not VEGFR-2 Ab, restored TEER to values very similar to the controls at all

incubation time (panel A). No significant change were observed in the TEER values after incubation of the co-cultures with VEGFR-1 Ab and VEGFR-2 Ab in absence of *E. coli* K1 (panels A and B). When co-cultures were infected with *E. coli* in the presence of AACOCF3 or BEL, TEER was restored by about 35% at 60 and 120 min (panel C). Regarding permeability studies, fluorescent intensity in the receiver chamber had already increased of about 2 fold after *E. coli* K1 incubation for 30 min (Fig. 9 D–F) and the fluorescence was more intense at each designated time point than untreated co-cultures. Incubation in the presence of VEGFR-1 Ab, but not VEGFR-2 Ab, attenuated of about 2.5-fold the diffusion of fluorescein sodium at each studied time (panels D and E). Moreover, when the cells were infected with *E. coli* K1 for 30, 60, 90 and 120 min in the presence of AACOCF3 or BEL, permeability was restored by about 44% in comparison with cells *E. coli* K1 in absence of PLA_2 inhibitors (panel F). The incubation of non-infected cells with AACOCF3 or BEL did not affect significantly TEER or permeability.

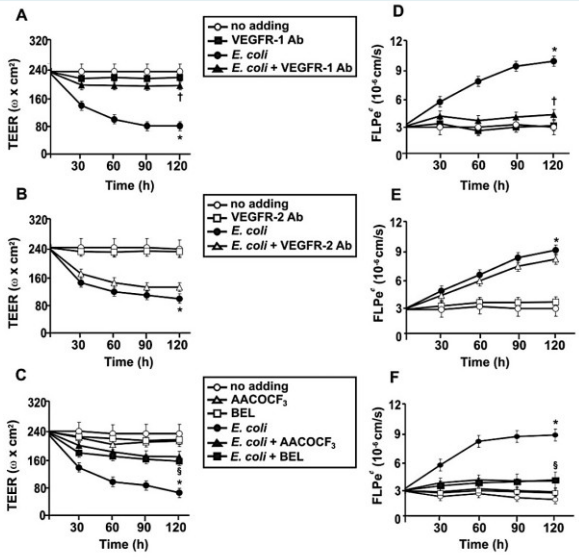

Fig. 9 – Role of PLA2 on barrier integrity during *E. coli* infection
Transendothelial electrical resistance (TEER) (A, B, C) and permeability to sodium fluorescein (D, E, F) of BBEC/BRPC co-culture on Transwell inserts after incubation with *E. coli* in absence or in presence of 2 mg ml-1 VEGFR-1 or 2 mg ml-1 VEGFR-2 antibodies, or 50 mM AACOCF3 or 2.5 mM BEL. Values are expressed as a mean SD of three independent experiments performed in triplicate. Statistically significant differences, by one-way ANOVA and the Tukey post-test ($P < 0.05$) are indicated as following: by asterisk (*), to compare stimulated *versus* control co-cultures (no adding bacteria); by dagger (†), to compare the statistically significant differences between *E. coli*-stimulated co-cultures in the presence of VEGFR-1 antibody versus the respective stimulated in the absence of VEGFR-1 antibody; by section symbol (§), to compare the statistically significant differences between *E. coli*-treated cells incubated with PLA2 inhibitors in comparison with the respective *E. coli*-treated ones in absence of inhibitors.

DISCUSSION

Neonatal *E. coli* meningitis is associated with significant morbidity and mortality. In order to reach the brain, circulating bacteria need to cross the BBB, consisting of brain microvascular EC that interact dynamically with other cells nearby, PC, astroglia, perivascular microglia and neurones (Ballabh *et al*., 2004).

PC communicate with EC releasing soluble factors responsible of the upregulation of BBB functions (Hori *et al*., 2004; Dohgu *et al*., 2005; 2011; Takata *et al*., 2007; Nakagawa *et al*., 2009). Despite the fact that they share a common basement membrane with EC, they were not studied in a co-culture BBB model to test the molecular mechanism of bacterial invasion. Lipopolysaccaride-induced sepsis in mice leads to detachment of brain PC from the basal lamina (Nishioku *et al*., 2009), suggesting that brain PC plays a crucial role in BBB integrity.In addition, the genetic animal models of progressive PC loss with age have shown that BBB integrity is determined by the amount of PC coverage of cerebral microvessels (Bell *et al*., 2010). Therefore, loss of PC in brain microvasculature is often linked to BBB dysfunction.

E. coli K1 exibits brain tropism (Presadarao *et al*., 1999) and it has been demonstrated that VEGFR-1 is involved in *E. coli* K1 invasion of human brain EC via recruitment of the PI3K/Akt pathway (Zhao *et al*., 2010).

By using TEM and SEM, we showed that *E. coli* K1 is able to adhere and enter BBEC, but not BRPC, by a vesicle-mediated mechanism and is able to induce PLA_2 activation and PGE2 synthesis, these latter contributing to BBB disruption. In fact, anti-inflammatory drugs are administered for palliative care and treatment during Gram-negative bacterial infection (Kim *et al*., 2009; Hulscher *et al*., 2010) and the elimination of PGE2 across the BBB is inhibited by either intracerebral or intravenous administration of antibiotics and by intracerebral administration of non-steroidal anti-inflammatory drugs as well (Akanuma *et al*., 2011).

BRPC secrete higher levels of VEGFR in basal conditions compared to BBEC, suggesting a

stabilizing role for BBEC. Treatment with AACOCF3 and BEL, as well as COX-2 inhibitor NS-392, reduces *E. coli* K1 induced VEGFA secretion of BBEC/BRPC co-cultures, indicating the involvement of PLA_2, AA production and its metabolization in eicosanoids in the production of VEGFA, in agreement with other studies (Pai *et al*., 2001). Other studies further confirmed the role of PLA_2 activation in secretion of VEGF (Bamba *et al*., 2000; Ottino *et al*., 2004; Barnett *et al*., 2010). Increase of BBB permeability could be related to PC coverage ablation due to PGs and VEGF biological effects on BBB.

In our model system, permeability increased within 30 min, suggesting that other factors may be involved in the increased permeability induced by VEGF. It is known that VEGF plays a key role in impairment of function of BBB (Murata *et al*., 1995; Hofman *et al*., 2000; 2001; Witmer *et al*., 2003), and activates pathways that were also activated during *E. coli* K1 invasion of microvascular endothelial cells (Zhao *et al*., 2010): VEGF induces tyrosine kinase receptor phosphorylation, internalization and cleavage of VE-cadherin, which can cause disruption of adherens junctions coupled with increase of vascular permeability (Dejana *et al*., 2008).

After *E. coli* K1 tratment of co-cultures with VEGFR-1 blocked in both cellular type or in co-cultures in which only BRPC, and not BBEC, were treated with VEGFR-1 Ab, the values of TEER and permeability to sodium fluorescein were very similar to those of non-infected co-cultures.

Moreover, the important role played by PLA_{2s} in maintaining barrier properties was demonstrated performing experiments in which we observed a rescue of almost 40% in TEER and permeability after *E. coli* K1 infection of co-cultures in presence of AACOCF3 or BEL in comparison with co-cultures infected with *E. coli* K1 in absence of PLA_2 inhibitors.

Zhao *et al*. (2010) already showed the involvement of VEGFR-1 during *E. coli* K1 invasion of brain endothelial, while Salmeri et al. (2019) demonstrated that c- and $iPLA_2$ activities and $cPLA_2$ phosphorylation were stimulated in microvascular endothelial cells after *E. coli* incubation and that PI3K and ERK 1/2 inhibitors reversed $cPLA_2$ phosphorylation (Salmeri *et al*., 2012). Arachidonic acid released after *E. coli* K1 infection could become the substrate of cyclooxygenases for the

production of PGs, whose could exert a proangiogenic influence by inducing VEGF secretion by endothelial cells. VEGF released by endothelial cells could target VEGFR-1 on the membrane of adjacent pericytes and determine their leak, acting as a negative regulator. The VEGF negative role on pericyte function was already shown in the C310T1/2 pericyte line, (Greenberg *et al*., 2008). It has also been showed that systemic administration of VEGF ablates pericytes from the mature retinal vasculature through the VEGFR-1 mediated signalling pathway, leading to increased vascular (Cao *et al*., 2010).

Results of this study show the defensive role played by the pericytes during a bacterial attack. The association of an antibiotic therapy with a drug able to block the VEGFR-1 on PC could represent a novel strategy against neonatal bacterial meningitis because would mean slowing down PC loss, thus protecting the anatomical integrity of the microvessels ans BBB overall.

Reference list, first study

Abbott N.J., Rönnbäck L., Hansson E. (2006) Astrocyte-endothelial interactions at the blood-brain barrier. *Nature Reviews Neuroscience* **7(1)**: 41-53.

Abbott N.J., Patabendige A.A., Dolman D.E., Yusof S.R., Begley D.J. (2010) Structure and function of the blood-brain barrier. *Neurobiol Dis* **37(1)**:13-25.

Akanuma, S., Hosoya, K., Ito, S., Tachikawa, M., Terasaki, T., and Ohtsuki, S. (2010) Involvement of multidrug resistance-associated protein 4 in efflux transport of prostaglandin E2 across mouse blood–brain barrier and its inhibition by intravenous administration of cephalosporins. *J Pharmacol Exp Ther* **333:** 912–919.

Akanuma, S., Uchida, Y., Ohtsuki, S., Tachikawa, M., Terasaki, T., and Hosoya, K. (2011) Attenuation of prostaglan- din E2 elimination across the mouse blood–brain barrier in lipopolysaccharide-induced inflammation and additive inhibitory effect of cefmetazole. *Fluids Barriers CNS* **8:** 24.

Alberghina, M. (2010) Phospholipase A(2): new lessons from endothelial cells. *Microvasc Res* **80:** 280–285.

Anfuso, C.D., Lupo, G., Romeo, L., Giurdanella, G., Motta, C., Pascale, A., *et al*. (2007) Endothelial cell-pericyte cocultures induce PLA2 protein expression through activation of PKCalpha and the MAPK/ERK cascade. *J Lipid Res* **48:** 782–793.

Armulik, A., Genové, G., Mäe, M., Nisancioglu, M.H., Wallgard, E., Niaudet, C., *et al*. (2010) Pericytes regulate the blood–brain barrier. *Nature* **468:** 557–561.

Ballabh, P., Braun, A., and Nedergaard, M. (2004) The blood– brain barrier: an overview. Structure, regulation and clinical implications. *Neurobiol Dis* **16:** 1– 13

Bamba, H., Ota, S., Kato, A., Kawamoto, C., and Fujiwara, K. (2000) Prostaglandins up-regulate vascular endothelial growth factor production through distinct pathways in differentiated U937 cells. *Biochem Biophys Res Commun* **273:** 485–491.

Barnett, J.M., McCollum, G.W., and Penn, J.S. (2010) Role of cytosolic phospholipase A(2) in retinal neovascularization. *Invest Ophthalmol Vis Sci* **51:** 1136–1142.

Bauer, H., Zweimueller-Mayer J., et al. (2010) The dual role of zonula occludens (ZO) proteins. *J Biomed Biotechnol* **2010**: 402593.

Bell R.D. and Zlokovic B.V. (2009). Neurovascular mechanisms and blood-brain barrier disorder in Alzheimer's disease. *Acta Neuropathol* **118(1)**: 103-13.

Bell, R.D., Winkler, E.A., Sagare, A.P., Singh, I., LaRue, B., Deane, R., and Zlokovic, B.V. (2010) Pericytes control key neurovascular functions and neuronal phenotype in the adult brain and during brain aging. *Neuron* **68:** 409–427.

Bergers G., Song S. (2005) The role of pericytes in blood-vessel formation and maintenance *Neuro Oncol* **7**:452-464.

Bonkowski, D., Katyshev, V., Balabanov, R.D., Borisov, A., and Dore-Duffy, P. (2011) The CNS microvascular pericyte: pericyte-astrocyte crosstalk in the regulation of tissue survival. *Fluids Barriers CNS* **8:** 8.

Cao, R., Xue, Y., Hedlund, E.M., Zhong, Z., Tritsaris, K., Tondelli, B., *et al*. (2010) VEGFR1-mediated pericyte ablation links VEGF and PlGF to cancer-associated retinopathy. *Proc Natl Acad Sci USA* **107:** 856–861.

Chen, Y., Merzdorf C., et al. (1997). COOH terminus of occludin is required for tight junction barrier function in early Xenopus embryos. *J Cell Biol* **138(4)**: 891-9.

Cogen A.L., Nizet V., Gallo R.L. (2008) Skin microbiota: a source of disease or defense? *Br J Dermatol* **158(3)**:442-455.

Dando S.J., Mackay-Sim A., Norton R. et al. (2014) Pathogens penetrating the Central Nervous System: infection pathways and the cellular and molecular mechanisms of invasion. *Clin Microbiol Rev* **27(4)**:691-726.

Daneman R., Zhou L., Kebede A.A. et al. (2010) Pericytes are required for blood-brain barrier integrity during embryogenesis. *Nature* **468**(7323):562-6.

Dauchy, S., Dutheil F. (2008). ABC transporters, cytochromes P450 and their main transcription factors: expression at the human blood-brain barrier. *J Neurochem* **107(6)**: 1518-28.

Dejana, E., Orsenigo, F., and Lampugnani, M.G. (2008) The role of adherens junctions and VE-cadherin in the control of vascular permeability. *J Cell Sci* **121:** 2115–2122.

Dìaz-Flores L., Gutiérrez R., Madrid J.F. et al. (2009) Pericytes. Morphofunction, interactions and pathology in a quiescent and activated mesenchymal cell niche. *Histol Histopathol* **24(7)**:909-69.

Dohgu, S., Takata, F., Yamauchi, A., Nakagawa, S., Egawa, T., Naito, M., *et al*. (2005) Brain pericytes contribute to the induction and up-regulation of blood–brain barrier functions through transforming growth factor-beta production. *Brain Res* **1038:** 208–215.

Dohgu, S., Takata, F., Matsumoto, J., Oda, M., Harada, E., Watanabe, T., *etal*. (2011) Autocrine and paracrine up-regulation of blood–brain barrier function by plasminogen activator inhibitor-1. *Microvasc Res* **81:** 103–107.

Dore-Duffy, P. (2008) Pericytes: pluripotent cells of the blood brain barrier. *Curr Pharm Des* **14:** 1581–1593.

Ehrlich P. (1885) Sauerstoff-Bedürfniss des Organismus Eine farbenanalytische Studie.

Engblom, D., Ek, M., Saha, S., Ericsson-Dahlstrand, A., Jakobsson, P.J., and Blomqvist, A. (2002) Prostaglandins as inflammatory messengers across the blood–brain barrier. *J Mol Med* **80:** 5–15.

Esser, S., Lampugnani, M.G., Corada, M., Dejana, E., and Risau, W. (1998) Vascular endothelial growth factor induces VE-cadherin tyrosine phosphorylation in endothelial cells. *J Cell Sci* **111:** 1853–1865.

Evan der Flier, M., Stockhammer, G., Vonk, G.J., Nikkels, P.G., van Diemen-Steenvoorde, R.A., van der Vlist, G.J., *et al*. (2001) Vascular endothelial growth factor in bacterial men- ingitis: detection in cerebrospinal fluid and localization in postmortem brain. *J Infect Dis* **183:** 149–153.

Feldman, G. J., Mullin J.M., et al. (2005). Occludin: structure, function and regulation. *Adv Drug Deliv Rev* **57(6)**: 883-917.

Ferrara N. and Kerbel R. (2005) Angiogenesis as a therapeutic target. *Nature* **438**: 967-974.

Ferrara N. and Adamis A. (2016) Ten years of anti-vascular endothelial growth factor therapy. *Nature Reviews Drug Discovery* **15**: 385-403.

Gerhardt H., Betsholtz C. (2003) Endothelial-pericyte interactions in angiogenesis *Cell Tissue Res*. **314**:15-23.

Giurdanella, G., Motta, C., Muriana, S., Arena, V., Anfuso, C.D., Lupo, G., and Alberghina, M. (2011) Cytosolic and calcium-independent phospholipase A2 mediate glioma-enhanced proangiogenic activity of brain endothelial cells. *Microvasc Res* **81:** 1–17.

Gliki, G., Abu-Ghazaleh, R., Jezequel, S., Wheeler-Jones, C., and Zachary, I. (2001) Vascular endothelial growth factor-induced prostacyclin production is mediated by a protein kinase C (PKC)-dependent activation of extracellu- lar signal-regulated protein kinases 1 and 2 involving PKC-delta and by mobilization of intracellular Ca2+. *Biochem J* **353:** 503–512.

Goldmann E.E. (1909) Die äussere und Sekretion des gesunden und kranken Organismus im Lichte der "vitalen Färbung". *Beitr Klin Chirurz* **64**:192–265.

Gumbiner, B., Lowenkopf T., et al. (1991). Identification of a 160-kDa polypeptide that binds to the tight junction protein ZO-1. *Proc Natl Acad Sci* **88(8)**: 3460-4.

Haddad-Tòvolli R., Dragano N.R., Ramalho A.F.S. et al. (2017) Development and function of the Blood-Brain Barrier in the context of metabolic control. *Front Neurosci* **11**:224.

Hamilton, N. B., Attwell D. (2010) Pericyte-mediated regulation of capillary diameter: a component of neurovascular coupling in health and disease. *Front Neuroenergetics* **21**;2.

Han H.S. and Suk K. (2005) The function and integrity of the neurovascular unit rests upon the integration of the vascular and inflammatory cell systems. *Curr Neurovasc Res* **2**:409-423.

Hawkins B.T, Davis T.P. (2005) The blood brain barrier/neurovascular unit in health and disease. *Pharmacol Rev* **57(2)**:173-85.

Hirase T., Staddon J.M., Saitou M. et al. (1997) Occludin as a possible determinant of tight junction permeability in endothelial cells. *J Cell Sci* **110**:1603-13.

Hoffman O. and Weber R.J. (2009). Pathophysiology and treatment of bacterial meningitis. *Ther Adv Neurol Disord* **2(6):**1-7.

Hofman, P., Blaauwgeers, H.G., Tolentino, M.J., Adamis, A.P., Nunes Cardozo, B.J., Vrensen, G.F., and Schlinge- mann, R.O. (2000) VEGF-A induced hyperpermeability of blood-retinal barrier endothelium *in vivo* is predominantly associated with pinocytotic vesicular transport and not with formation of fenestrations. Vascular endothelial growth factor-A. *Curr Eye Res* **21:** 637–645.

Hofman, P., van Blijswijk, B.C., Gaillard, P.J., Vrensen, G.F., and Schlingemann, R.O. (2001) Endothelial cell hypertrophy induced by vascular endothelial growth factor in the retina: new insights into the pathogenesis of capillary non-perfusion. *Arch Ophthalmol* **119:** 861–866.

Hom, S., Fleegal M.A., et al. (2007). Comparative changes in the blood-brain barrier and cerebral infarction of SHR and WKY rats. *Am J Physiol Regul Integr Comp Physiol* **292(5)**: R1881-92.

Hori, S., Ohtsuki, S., Hosoya, K., Nakashima, E., and Tera- saki, T. (2004) A pericyte-derived angiopoietin-1 multimeric complex induces occludin gene expression in brain capil- lary endothelial cells through Tie-2 activation *in vitro*. *J Neurochem* **89:** 503–513.

Hulscher, M.E., Grol, R.P., and van der Meer, J.W. (2010) Antibiotic prescribing in hospitals: a social and behavioural scientific approach. *Lancet Infect Dis* **10:** 167–175.

Inoko, A., Itoh M., et al. (2003). Expression and distribution of ZO-3, a tight junction MAGUK protein, in mouse tissues. *Genes Cells* **8(11)**: 837-45.

Janzer, R.C. and Raff M.C. (1987). Astrocytes induce blood-brain barrier properties in endothelial cells. *Nature* **325(6101)**: 253-7.

Jia W., Martin T.A., Zhang G. et al. (2013) Junctional adhesion molecules in cerebral endothelial tight junction and brain metastasis. *Anticancer Res* **33(6):**2353-9.

Kajdaniuk, D., Marek, B., Foltyn, W., and Kos-Kudła, B. (2011) Vascular endothelial growth factor (VEGF) – part 1: in physiology and pathophysiology. *Endokrynol Pol* **62:** 444–455.

Kim, K.S. (2003) Pathogenesis of bacterial meningitis: from bacteraemia to neuronal injury. *Nat Rev Neuroscience* **4:** 376–385.

Kim, K.S. (2008) Mechanisms of microbial traversal of the blood–brain barrier. *Nat Rev Microbiol* **6:** 625–634.

Kim, S.Y., Chang, Y.J., Cho, H.M., Hwang, Y.W., and Moon, Y.S. (2009) Non-steroidal antiinflammatory drugs for the common cold. *Cochrane Database Syst Rev* (3)**:** CD006362.

Kong, J.S., Yoo, S.A., Kang, J.H., Ko, W., Jeon, S., Chae, C.B., *et al*. (2011) Suppression of neovascularization and experimental arthritis by d-form of anti-flt-1 peptide conjugated with mini-PEG(TM). *Angiogenesis* **14:** 431– 442.

Krishnan, S., Fernandez, G.E., Sacks, D.B., and Prasadarao, N.V. (2012) IQGAP1 mediates the disruption of adherens junctions to promote *Escherichia coli* K1 invasion of brain endothelial cells. *Cell Microbiol* **14:** 1415–1433.

Lippoldt, A., Liebner S., et al. (2000). Organization of choroid plexus epithelial and endothelial cell tight junctions and regulation of claudin-1, -2 and -5 expression by protein kinase C. *Neuroreport* **11(7):** 1427-31.

Lupo, G., Anfuso, C.D., Ragusa, N., Strosznajder, R.P., Walski, M., and Alberghina, M. (2001) t-Butyl hydroperoxide and oxidized low density lipoprotein enhance phos- pholipid hydrolysis in lipopolysaccharide-stimulated retinal pericytes. *Biochim Biophys Acta* **1531:** 143–155.

Lupo, G., Assero, G., Anfuso, C.D., Nicotra, A., Palumbo, M., Cannavò, G., *et al*. (2002) Cytosolic phospholipase A2 mediates arachidonoyl phospholipid hydrolysis in immortalized rat brain endothelial cells stimulated by oxidized LDL. *Biochim Biophys Acta* **1585:** 19–29.

Mi, H., Haeberle H., et al. (2001). Induction of astrocyte differentiation by endothelial cells. *J Neurosci* **21(5)**: 1538-47.

Miller, D. S. (2010) Regulation of P-glycoprotein and other ABC drug transporters at the blood-brain barrier. *Trends Pharmacol Sci* **31(6)**: 246-54.

Murata, T., Ishibashi, T., Khalil, A., Hata, Y., Yoshikawa, H., and Inomata, H. (1995) Vascular endothelial growth factor plays a role in hyperpermeability of diabetic retinal vessels. *Ophthalmic Res* **27:** 48–52.

Nakagawa, S., Deli, M.A., Kawaguchi, H., Shimizudani, T., Shimono, T., Kittel, A., *et al*. (2009) A new blood–brain barrier model using primary rat brain endothelial cells, pericytes and astrocytes. *Neurochem Int* **54:** 253– 263.

Nico, B., and Ribatti, D. (2012) Morphofunctional aspects of the blood–brain barrier. *Curr Drug Metab* **13:** 50–60. Nishioku, T., Dohgu, S., Takata, F., Eto, T., Ishikawa, N., Kodama, K.B., *et al*. (2009) Detachment of brain pericytes from the basal lamina is involved in disruption of the blood–brain barrier caused by lipopolysaccharide-induced sepsis in mice. *Cell Mol Neurobiol* **29:** 309–316.

Ohtsuki S., Terasaki T. (2007) Contribution of carrier-mediated transport systems to the blood-brain barrier as a supporting and protecting interface for the brain; importance for CNS drug discovery and development. *Pharm Res* 24(9):1754-58.

Ottino, P., Finley, J., Rojo, E., Ottlecz, A., Lambrou, G.N., Bazan, H.E., and Bazan, N.G. (2004) Hypoxia activates matrix metalloproteinase expression and the VEGF system in monkey choroid-retinal endothelial cells: involvement of cytosolic phospholipase A2 activity. *Mol Vis* **10:** 341–350.

Pai, R., Szabo, I.L., Soreghan, B.A., Atay, S., Kawanaka, H., and Tarnawski, A.S. (2001) PGE(2) stimulates VEGF expression in endothelial cells via ERK2/JNK1 signaling pathways. *Biochem Biophys Res Commun* **286:** 923– 928.

Pardridge W.M. (2001) Brain drug targeting: the future of brain drug development *Cambridge Univ Pr*.

Presadarao, N.V., Wass, C.A., Stins, M.F., Shimada, H., and Kim, K.S. (1999) Outer membrane protein A-promoted actin condensation of brain microvascular endothelial cells is required for *Escherichia coli* invasion. *Infect Immun* **67:** 5775–5783.

Reese, T. S. and M. J. Karnovsky (1967). Fine structural localization of a blood-brain barrier to exogenous peroxidase. *J Cell Biol* **34(1)**: 207-17.

Ribatti D., Nico B., Crivellato E., Artico M. (2006) Development of the blood-brain barrier: A historical point of view. *The Anatomical Record Part B: The New Anatomist* **289(1)**: 3-8.

Ronaldson, P.T. Babakhanian K., and Bendayan R. (2007) Drug Transport in the Brain. Edited by G. You and M.E. Morris in Molecular Characterization and role of Drug Disposition: 412-460.

Rubin, L.L., Hall D.E., et al. (1991). A cell culture model of the blood-brain barrier. *J Cell Biol* **115(6)**: 1725-35.

Salcedo, R., and Oppenheim, J.J. (2003) Role of chemokines in angiogenesis: CXCL12/SDF-1 and CXCR4 interaction, a key regulator of endothelial cell responses. *Microcirculation* **10:** 359–370.

Salmeri, M., Motta, C., Mastrojeni, S., Amodeo, A., Anfuso, C.D., Giurdanella, G., *etal*. (2012) Involvement of PKCa-MAPK/ERK-phospholipase A(2) pathway in the *Escherichia coli* invasion of

brain microvascular endothelial cells. *Neurosci Lett* **511:** 33–37.

Sá-Pereira, I., Brites, D., and Brito, M.A. (2012) Neurovascu- lar unit: a focus on pericytes. *Mol Neurobiol* **45:** 327–347. Stanimirovic, D.B., and Friedman, A. (2012) Pathophysiology of the neurovascular unit: disease cause or consequence? *J Cereb Blood Flow Metab* **32:** 1207–1221.

Severson, E.A. and Parkos C.A. (2009). Structural determinants of Junctional Adhesion Molecule A (JAM-A) function and mechanisms of intracellular signaling. *Curr Opin Cell Biol* **21(5)**: 701-7.

Stevenson, B. R., Siliciano J.D., et al. (1986). Identification of ZO-1: a high molecular weight polypeptide associated with the tight junction (zonula occludens) in a variety of epithelia. *J Cell Biol* **103(3)**: 755-66.

Stewart, P. A. and Wiley M.J. (1981). Developing nervous tissue induces formation of blood-brain barrier characteristics in invading endothelial cells: a study using quail--chick transplantation chimeras. *Dev Biol* **84(1)**: 183-92.

Subramanian, J., Morgensztern, D., and Govindan, R. (2010) Vascular endothelial growth factor receptor tyrosine kinase inhibitors in non-small-cell lung cancer. *Clin Lung Cancer* **11:** 311–319.

Sukumaran, S.K., Quon, M.J., and Prasadarao, N.V. (2002) *Escherichia coli* K1 internalization via caveolae requires caveolin-1 and protein kinase Calpha interaction in human brain microvascular endothelial cells. *J Biol Chem* **277:** 50716–50724.

Tait, M.J., Saadoun S., et al. (2008). Water movements in the brain: role of aquaporins. *Trends Neurosci* **31(1)**: 37-43.

Takata, F., Dohgu, S., Yamauchi, A., Sumi, N., Nakagawa, S., Naito, M., *et al*. (2007) Inhibition of transforming growth factor-beta production in brain pericytes contributes to cyclosporin A-induced dysfunction of the blood–brain barrier. *Cell Mol Neurobiol* **27:** 317–328.

Takenaga, Y., Takagi N., et al. (2009). Inhibition of Src activity decreases tyrosine phosphorylation of occludin in brain capillaries and attenuates increase in permeability of the blood-brain barrier after transient focal cerebral ischemia. *J Cereb Blood Flow Metab* **29(6)**: 1099-108.

Wheeler-Jones, C., Abu-Ghazaleh, R., Cospedal, R., Houlis- ton, R.A., Martin, J., and Zachary, I. (1997) Vascular endothelial growth factor stimulates prostacyclin production and activation of cytosolic phospholipase A2 in endothelial cells via p42/p44 mitogen-activated protein kinase. *FEBS Lett* **420:** 28–32.

Winkler, E.A., Bell, R.D., and Zlokovic, B.V. (2011) Central nervous system pericytes in health and disease. *Nat Neu- rosci* **14:** 1398–1405.

Witmer, A.N., Vrensen, G.F., Van Noorden, C.J., and Schlingemann, R.O. (2003) Vascular endothelial growth factors and angiogenesis in eye disease. *Prog Retin Eye Res* **22:** 1–29.

Zhao, W.D., Liu, W., Fang, W.G., Kim, K.S., and Chen, Y.H. (2010) Vascular endothelial growth factor receptor 1 con- tributes to *Escherichia coli* K1 invasion of human brain microvascular endothelial cells through the phosphatidylinositol 3-kinase/Akt signaling pathway. *Infect Immun* **78:** 4809–4816.

Zhu, L., Pearce, D., and Kim, K.S. (2010a) Prevention of *Escherichia coli* K1 penetration of the blood–brain barrier by counteracting the host cell receptor and signaling mol- ecule involved in *E.*

coli invasion of human brain microvascular endothelial cells. *Infect Immun* **78:** 3554–3559.

Zhu, L., Maruvada, R., Sapirstein, A., Malik, K.U., Peters- Golden, M., and Kim, K.S. (2010b) Arachidonic acid metabolism regulates *Escherichia coli* penetration of the blood–brain barrier. *Infect Immun* **78:** 4302–4310.

Zimmermann K.W. (1923) Der feinere bau der blutcapillares, *Z. Anat. Entwicklungsgesch* 68: 3-109.

Zlokovic, B. V. (2008). The blood-brain barrier in health and chronic neurodegenerative disorders. *Neuron* **57(2)**: 178-201.

BACKGROUND: second study

As already discussed, TJs seal BMECs each other and depend on the presence of proteins such as Claudins, Occludin, β-catenin and cytoplasmic ZO proteins to create a continuous sheet covering the inner surface of microcapillaries (Abbott *et al.*, 2010). When TJs expression is reduced, BBB permeability increases (Dejana *et al.*, 2009). BMPCs are located on abluminal surface of the endothelium and orchestrate many neurovascular functions, such as BBB formation and regulation of capillary blood flow (Winkler *et al.,* 2011). Moreover, pericytes possess features of multipotent cells and therefore and great potential for therapy have been addressed on them (Dore-Duffy, 2008). Despite pivotal roles exerted by BMPCs, less is known about the mechanisms by which vasoactive molecules, such as adenosine, regulate their physiological function.

Adenosine derives from the catabolism of extracellular adenosine triphosphate (ATP).

Role and metabolism of adenosine

In physiological conditions, adenosine exerts beneficial anti-inflammatory effects. Conversely, chronic elevation of adenosine levels is present during pathological conditions characterized by inflammation (Borea *et al.*, 2017). After an insult to the cellular membrane, the cell release high concentrations of ATP, that is first converted into adenosine diphosphate (ADP) and adenosine monophosphate (AMP) by CD39 extracellular enzyme; then, CD73 extracellular enzyme will convert AMP to adenosine (Borea *et al.*, 2017).

Adenosine receptors

Adenosine binds its receptors (ARs), which are purinergic G protein-coupled receptors. There are four different subtypes of ARs, A_1, A_{2A}, A_{2B} and A_3. A_1 and A_3 receptors induce an inhibition of adenylyl ciclase through $G_{i/o}$ protein family, thus reducing intracellular levels of cAMP whereas A_{2A} and A_{2B} activate cAMP synthesis via G_s. Moreover, A_1 and A_{2A} have high affinity whereas A_3 and A_{2B} have low affinity for adenosine (Do-Geun *et al*., 2015). It has been demonstrated that ARs and extracellular enzymes are expressed in brain endothelial cells in mice and humans and that CD73 expression is very low and not detectable in vivo (Do-Geun *et al*., 2015). It has also been demonstrated that the activation of ARs with AR agonists increased BBB permeability by reducing TJ protein expression (Bynoe et al., 2015; Carman et al., 2011) indicating that these agonists are able to control the entry of different molecules into the CNS. Recent studies demonstrated that the permeability process, induced by A_{2A}-AR activation, is mediated by Rho signalling pathway (Denk-Lobnig *et al.*, 2017).

An important role in infection disease progression is played by adenosine A_{2B} receptors, as demonstrated by studies conducted on a murine model infected by *C. difficile* (Warren *et al.*, 2012) and on HeLa cells after chlamydial infection (Pettengill *et al.*, 2012). Souza *et al.* demonstrated the involvement of both A_{2A} and A_{2B} adenosine receptors in increased MMP-9 secretion in *S. aureus* infected macrophages (Souza *et al.*, 2009). Based on these studies, we focused our attention on determining whether *Haemophilus influenzae* (Hi) can modulate the BBB permeability through A_{2A} and A_{2B} -ARs to enter BMECs.

HAEMOPHILUS INFLUENZAE MENINGITIS

Haemophilus influenzae

Hi is an important human-restricted Gram-negative pathogen, which normally resides in the upper respiratory tract of humans and can cause severe localized (otitis media, sinusitis) and systemic (bacteremia, meningitis, pneumonia, septic arthritis, epiglottitis) infections in susceptible individuals (Stefani *et al.*, 2008). Some strains of Hi have a polysaccharide capsule representing the major virulence factor and antigen of this bacterial species. On the basis of its antigenic properties, six serotypes of encapsulated Hi are distinguishable (a, b, c, d, e, and f), and there are also non-encapsulated or non-typeable Hi (NTHi). Encapsulated strains exhibit a higher ability to cause invasive disease because the capsule prevents complement-mediated bacteriolysis in the absence of opsonizing antibodies (Prajapati et al., 2017).

Haemophilus influenzae, serotype b

Of the six serotypes, serotype b (Hib) was a common cause of childhood meningitis before the Hib conjugate vaccine was introduced (Slack, 2006).

Despite the widespread use of vaccines, several populations remain vulnerable to Hib disease even with vaccination (Zarei *et al.*, 2016). Moreover, Hib vaccination does not confer protection against other serotypes of Hi. Other serological types of Hi, besides Hib, cause significant morbidity and mortality and their prevalence appears to be increasing in the Hib vaccine era (Zarei *et al.*, 2016).

Haemophilus influenzae, serotype a

Non-Hib diseases are becoming an emergenzy worldwide; likely Hib, of Hi serotype a (Hia) capsule represents an important virulence factor contributing to development of invasive disease (Ulanova *e al.*, 2009). It is unknow if the emergence of invasive Hia disease is due to the serotype

replacement after the wide use of Hib vaccine for child immunization (Ulanova *et al.*, 2014; Ladhani *et al.*, 2010). Given that Hia disease did not received adequate surveillance worldwide, it is now recognized as a pathogen responsible of serious diseases comparable to Hib in severity and case-mortality rates (Lima *et al.*, 2010; Gona *et al*., 2014; Jin *et al*., 2007) and deserving of interest to understand the evolving nature of the disease both to control the development of infection and for prevention. So far, no *in vitro* studies are conducted to clarify the mechanisms by which Hia, which colonizes the upper respiratory tract, is able to cross BBB, leading to meningitis.

AIM OF THE STUDY

Despite the progresses of antimicrobial treatments, bacterial meningitis remain infection of the CNS with high morbidity and mortality, (Kim, 2008). It is known that the bacteria can leave the principal organ of infection by using the blood flux and, as circulating bacteria, reach and cross BBB leading to meningitis (Kim, 2003).

By using an *in vitro* model of BBB, made of hBMECs and hBMPCs in co-culture, we have hypothesized that Hia-infected endothelial cells release high amount of adenosine, which binds A_{2B} –ARs on hBMECs and hBMPCs, triggering VEGF release, responsible for BBB breakdown.

MATERIAL AND METHODS

All reagents and antibodies were purchased from Sigma (St. Louis, MO) or E. Merck (Darmstadt, Germany) unless otherwise indicated. Antibodies against α actin, NG2, Von Willebrand factor, VE-Cadherin, CREB, phosphorylated CREB, Rho-A and phosphorylated Rho-A were from Santa Cruz Biotechnology Inc. (CA).

Cell cultures

Primary human brain microvascular endothelial cells (hBMECs) and human brain microvascular pericytes (hBMPCs) were purchased from Innoprot and fed with basal medium supplemented with 5% fetal bovine serum (FBS), 100 U/ml penicillin, 100 μg/ml streptomycin, and 1% endothelial cell growth supplement (ECGS).

Construction of *in vitro* BBB model

Transwell inserts (Transwells, Corning, Corning, NY) were coated on the upper and bottom side with 2 mg/ml solution of rat tail collagen before being placed in complete medium (half and half DMEM/HAM's). To construct an *in vitro* model of BBB, BRPC (2×10^4 cells cm^2) were first plated on the outside of the Transwell inserts membrane and placed upside down in the well culture plate to allow adhesion. After adhesion, the Transwells were inverted and BBEC (2×10^4 cells cm^2) were seeded on the top surface of the insert. Under these conditions, the two type of cells on direct contact established an *in vitro* BBB model within 3 days.

H. influenzae preparation and infection

Hia strain (NCTC 8466, type a) was grown in chocolate agar (Difco, Sparks, MD) for 24 h at 37°C in an atmosphere enriched with CO_2 before to be harvested, suspended in 0.5 ml of PBS (Gibco, Invitrogen, Carlsbad, CA) and serially diluted to the needed concentration.

After reaching confluence, FBS-containing medium was removed from hBMECs and hBMPCs in monoculture and in co-culture, and serum-free medium was added 4h before infection with Hia (10^7 CFU/well). After infection with bacteria, the co-cultures were washed three times with PBS, and hBMECs and hBMPCs were collected separately by trypsinization.

Electron microscopy

For Scanning Electron Microscopy (SEM) preparations, cells grown in co-colture on filters were fixed with 1.5% glutaraldehyde overnight, following by an additional fix in 1% OsO4 (1 h). Then, cells on the membrane were dehydrated in graded ethanol, critical point dried, sputtered with 5 nm gold layer using an Emscope SM 300 (Emscope Laboratories, Ashford, UK) and observed using a Hitachi S-4000 (Hitachi High-Technologies America, Schaumburg, IL) field emission scanning electron microscope.

For Transmission Electron Microscopy (TEM), after dehydrating in a graded series of acetone, cells were embedded in Durcupan ACM (Fluka Chemika-Biochemika, Buchs, Switzerland). Ultrathin sections were cut using a Reichert Ultracut E microtome and double stained with uranyl acetate and lead citrate. Observations were carried out using a Hitachi H-7000 transmission electron microscope (Hitachi High-Technologies Europe GmbH, Krefeld, Germany).

Immunoblotting

The lysates of hBMECs and hBMPCs, grown in co-culture, control (uninfected) and incubated with Hia for 6h, were prepared for Western blotting. Membranes were incubated overnight at 4°C with primary monoclonal antibodies against β-actin, NG2, von Willebrand factor, VE-cadherin, CREB,

p-CREB, Rho-A and p-Rho-A (dilution, 1:1000) and then with a secondary antibody (dilution, 1:2000) for 1h at room temperature.

Fluorescence microscopy

To investigate changes in VE-cadherin in hBMECs in co-culture with hBMPCs, after 6h infection with Hia, hBMPCs, grown on one side of the filter, were scraped to leave only hBMECs. The filters with hBMECs were fixed by adding 4% paraformaldehyde, and processed for immunocytochemistry using anti-VE-cadherin antibody (dilution, 1:100) and, as a secondary antibody, green fluorescence-labeled fluorescein isothiocyanate (dilution, 1:1,000). Hoechst® 33342 nucleic acid stain, was used to highlight the nuclei. The distribution of immunocomplexes was observed by an epifluorescent microscopy using appropriate filters.

Evaluation of the barrier integrity

Millicell electrical resistance system (Millipore) was used to measure TEER. Values were expressed as Ω x cm^2 and were calculated by the following formula: (average resistance of experimental wells x average resistance of blank wells) x 0.33 (area of the Transwell membrane). To address the role of ARs in BBB dysfunction, experiments were carried out by incubating the co-cultures, in presence or in absence of Hia infection, with 1 μM 8-[4-[4-(4-Chloro-phenzyl) piperazide-1-sulfonyl) phenyl]]-1-propylxanthine (PSB 603), a specific A_{2B} adenosine receptor antagonist or with 1 μM 2-(2-Furanyl)-7-(2-phenylethyl)-7H-pyrazolo[4,3-e][1,2,4] triazolo[1,5-c]pyrimidin-5-amine (SCH58261), a specific A_{2A} adenosine receptor antagonist or with 1 μM 8-cyclopentyl-l,3- dipropylxanthine (DPCPX), a specific A_1 adenosine receptor antagonist. In parallel, co-cultures were treated with 1 μM 2-Chloro-N6-cclopentyladenosine (CCPA), a specific A_1 adenosine receptor agonist or with 1 μM 2-(2-carboxyethyl)- phenethyl-amino-5'-N-ethylcarbox-amidoadenosine (CGS 21680), a specific A_{2A} adenosine receptor agonist or with 1 μM

5'-(N-ethylcar-boxamido)-adenosine (NECA), a generic A_2 adenosine receptor agonist in absence of Hia infection.

Moreover, TEER was measured after blocking of VEGFR-1 and VEGFR-2 by their specific antibodies (Ab) in both hBMECs and in hBMPCs in co-culture. For these simultaneous blockade experiments, co-cultures were treated with 2 μg/ml VEGFR1 or 2 μg/ml VEGFR2 Abs for 60 min before 6h treatment with Hia.

Bacterial invasion assay

Incubations of bacteria (10^7 CFU/well) with hBMECs/hBMPCs co-culture were performed at 37°C for 1, 3, 6 and 9h to allow invasion to occur. At the end of the incubation times, hBMECs were removed from the filter and the number of intracellular bacteria was determined after incubation with gentamicin (100 μg/ml) for 1 h at 37°C to kill all extracellular bacteria. Cells were then lysed with 0.5% Triton X-100 and lysates were seeded on chocolate agar plates to be numbered the day after. The results were expressed as percent invasion [100 x (number of intracellular bacteria recovered)/(number of bacteria inoculated)].

Cell viability

The number and viability of hBMECs/hBMPCs co-cultures after Hia infection for 1-3-6 and 9h was determined by trypan blue dye. Cells from inserts were trypsinized separately, cell suspensions were mixed with a 0.4% trypan blue solution, and the number of live cells was determined using a hemocytometer.

ENTPDase enzymatic activity assay

ENTPDase/5-nucleotidase enzymatic activity was determined by the release of inorganic phosphate (Pi). Briefly, 1×10^5 hBMEC or hBMPC in monoculture, or hBMEC/hBMPC co-cultures, infected

or non infected, were washed 3 times with phosphate-free buffer and pre-incubated in 100 □ L buffer in a 96-well microplate at 37°C for 30 min. To distinguish between CD37 and CD73 activity, 200 □ M ARL67156, a CD39-specific inhibitor, or 100 □ M methylene adenosine-5′-diphosphate (APCP), a CD73-specific inhibitor, was added. The release of Pi was determined by using the Malachite Green Phosphate Detection Kit (R&D Systems) according to the manufacturer's protocol.

cAMP Detection Assay

Total cAMP concentration was evaluated by using cAMP Biotrak Enzyme Immunoassay (Amersham Biosciences, Piscataway, NJ, USA). Control cells, non-infected, were incubated with forskolin (10 µmol/L). Mono- and co-cultures were infected 6h with Hia, in the absence or presence of SCH58261 (1 µM) or PSB603 (1 µM). After incubation, the two cell types were trypsinized separately from inserts and lysed for cAMP determination, following the manufacturer's protocols.

Statistical analysis

Statistical significance between two groups was analyzed by Student's test. One-way analysis of variance (ANOVA), followed by Tukey's *post hoc* test, was used to compare the mean for the multiple groups. *P* values < of 0.05 were considered statistically significant.

RESULTS

Bacterial invasion modified cell number

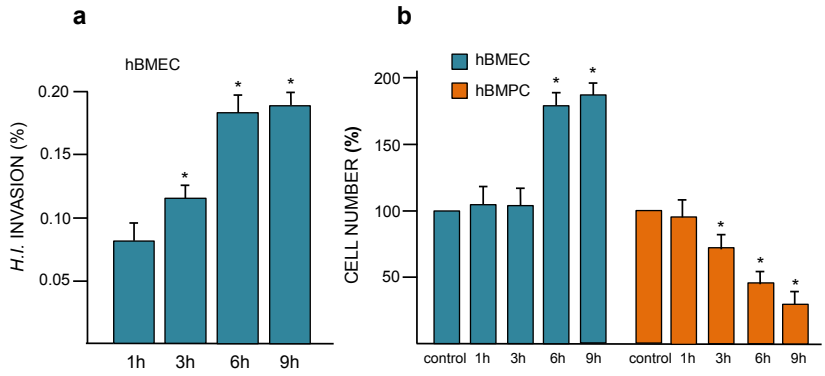

Figure 10. Panel a: invasion of hBMECs after incubation of the co-cultures for 1h, 3h, 6h, and 9h with *H. influenzae*. Values are expressed as a percentage of invasion ± SD by three independent experiments performed in triplicate. Statistically significant differences, by one-way ANOVA and the Tukey post-test are indicated (*p<0.05 *vs* 1h invasion). Panel c: number of live endothelial cells and pericytes, non-infected (control) and after 1h, 3h, 6h and 9h infection. Values, in percentage compared to control cells incubated in absence of bacteria (mean ± SD) are from three independent experiments (n=3). Statistically significant differences, by one-way ANOVA and the Tukey post-test are indicated (*p<0.05 *vs* the respective control).

Invasion after 3h and 6h of infection increased 1.5 and 2.2 fold, respectively, compared to invasion after 1h (Fig. 10, panel a), whereas the percentage of infection after 9h was similar to that of 6h, indicating that the majority of bacteria were able to enter cells after 6h of incubation. So, we have choosen 6h incubation for all the infection experiments. Trypan blue exclusion test showed that after 1h infection, cell viability was not affected (Fig. 10, panel b). After 3h, 6h and 9h of infection, hBMPCs number decreased 1.3-, 2.1- and 3.3 fold, respectively, compared to non-infected cells (control), whereas the number of endothelial cells after 6h and 9h infection increased 1.8- and 1.9 fold, in comparison with control cells. Probably, the increased endothelial cell numberis related to the detachment of pericytes which would no longer be able to control endothelial proliferation.

H. influenzae is able to enter hBMECs

Fig. 11, panel A, shows SEM images of hBMECs grown on Transwell filters at 6h post-infection

with Hia. In panels a and b, the endothelial cells at lower magnification show a thin phenotype with numerous microvilli on the surface and bacteria adhering in contact with them (black arrows). In panel c, bacteria are visible on the cell surface (black arrows) and through the cell membrane, suggesting that Hia were able to adhere and enter endothelial cells. In panel d, bacteria in contact with large pseudopodia are visible. In 11, panel B, TEM images of hBMECs infected 6h with Hia are shown. Panels a and b show numerous bacteria in contact with the surface of the cells by pili-like extensions containing microvilli and bacteria engulfed inside phagosomes. Many bacteria are present in the space between the endothelial cells because of the disruption of TJs.

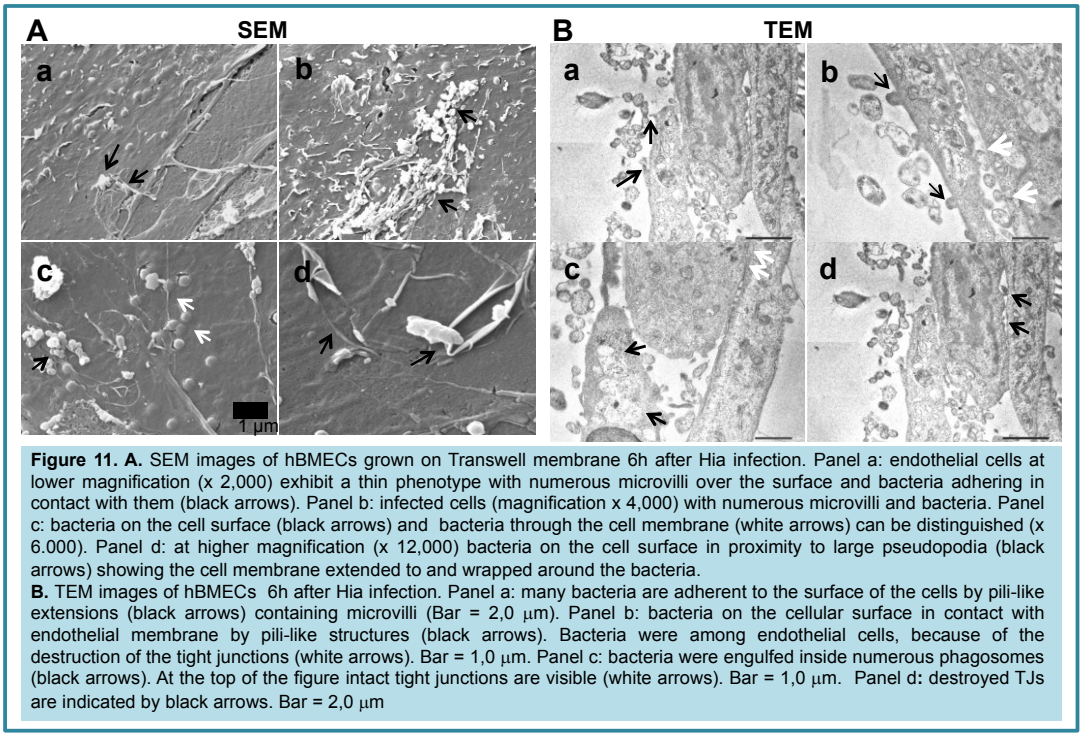

Figure 11. A. SEM images of hBMECs grown on Transwell membrane 6h after Hia infection. Panel a: endothelial cells at lower magnification (x 2,000) exhibit a thin phenotype with numerous microvilli over the surface and bacteria adhering in contact with them (black arrows). Panel b: infected cells (magnification x 4,000) with numerous microvilli and bacteria. Panel c: bacteria on the cell surface (black arrows) and bacteria through the cell membrane (white arrows) can be distinguished (x 6.000). Panel d: at higher magnification (x 12,000) bacteria on the cell surface in proximity to large pseudopodia (black arrows) showing the cell membrane extended to and wrapped around the bacteria.
B. TEM images of hBMECs 6h after Hia infection. Panel a: many bacteria are adherent to the surface of the cells by pili-like extensions (black arrows) containing microvilli (Bar = 2,0 µm). Panel b: bacteria on the cellular surface in contact with endothelial membrane by pili-like structures (black arrows). Bacteria were among endothelial cells, because of the destruction of the tight junctions (white arrows). Bar = 1,0 µm. Panel c: bacteria were engulfed inside numerous phagosomes (black arrows). At the top of the figure intact tight junctions are visible (white arrows). Bar = 1,0 µm. Panel d: destroyed TJs are indicated by black arrows. Bar = 2,0 µm

H. influenzae reduced TEER and VE-cadherin expression in hBMEC

Incubation of co-cultures for 1-6h with Hia significantly reduced TEER values (about 6.2 fold after 6h) compared to non-infected control co-cultures at the same time of incubation (Fig. 12, panel a). These results were confirmed by the fluorescence-microscopy images, where the distribution of fluorescent VE-cadherin was reduced in Hia infected cells compared to control cells (Fig. 12, panel b).

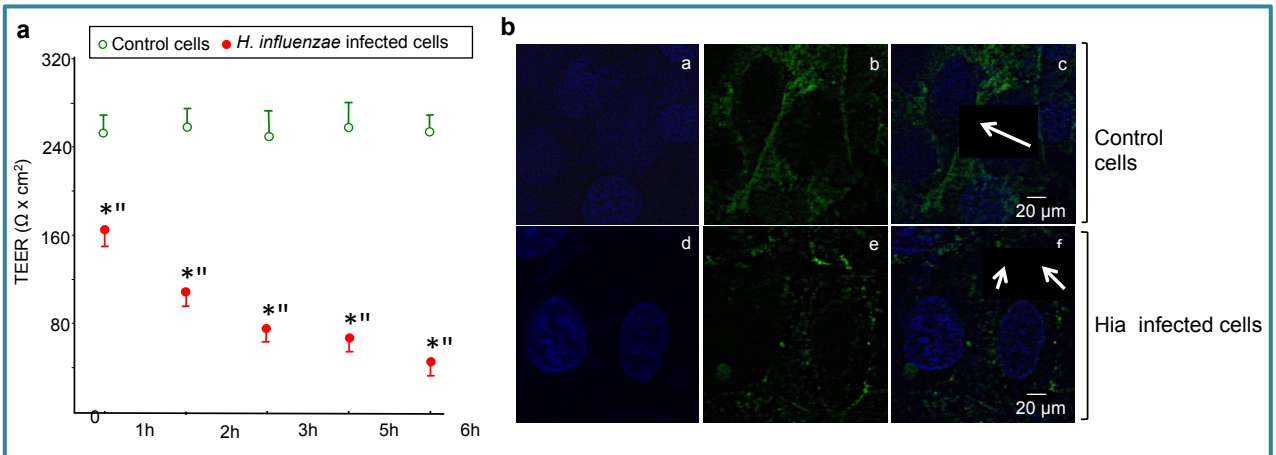

Figure 12. Panel a: TEER analysis: cells were incubated in absence or presence of Hia for 1, 2, 3, 5, 6 h. (n = 3). Statistically significant differences, by one-way ANOVA and the Tukey post-test are indicated (*p<0.05 vs control). Panel b: fluorescence microscopy images for expression of VE-Cadherin in hBMECs in co-culture with hBMPCs in absence or presence of Hia. Panels a and d: nuclei of live cells stained with Hoechst dye; panels b and e: VE-Cadherin stained with green fluorescent-labeled FITC; panels c and f: merge. Magnification x40.

Adenosine receptors were involved in *H. influenzae* infection

To deeper investigate the effect of adenosine, produced by infected endothelial cells, on close pericytes, TEER measurements after bacterial infection in presence of specific ARs antagonists was measured (Fig. 13). Bacterial infection significantly reduced TEER values (6.7 fold lower than control values after 6h, Fig. 13, panel a). Co-incubation of Hia with DPCPX, a specific A_1 adenosine receptor antagonist, did not change TEER values compared to 6h infected cells in absence of DPCPX. Conversely, cells co-incubated with Hia and SCH58261, a specific A_{2A} adenosine receptor antagonist, showed a significant increase of TEER values (4.1 fold) compared to 6h cells infected in absence of the antagonist. Even more surprisingly, a greater increase in TEER values was observed when Hia infection was performed together with PSB603 incubation, a specific A_{2B} adenosine receptor antagonist (5.4 fold increase), thus demonstrating that A_{2A} adenosine receptor and, more strongly, A_{2B} adenosine receptor play a pivotal role in BBB dysfunction during Hia infection. These results were confirmed cell count experients after Hia infection in presence of the above mentioned antagonists (Fig. 13, panel b). Infection of the co-cultures with Hia for 6h reduced the pericyte number (3.3 fold) and increase endothelial cell number (1.7 fold). Infection in presence of DPCPX reduced pericyte number and increased

endothelial cell number likewise to infected cells without antagonist. When the infection was carried out in presence of SCH58261 or PSB603, the pericyte number increased 2.6 fold and 3.0 fold, respectively, compared with the number of infected pericytes in absence of antagonists. Under the same experimental conditions, endothelial cell number decreased 1.5 fold and 1.4 fold, in presence of SCH58261 and in presence of PSB603, respectively, compared with the number of infected endothelial cells in absence of antagonists. Thus, Hia is able to increase adenosine concentration inside endothelial cells, within which it is able to penetrate to cross BBB and reach the SNC. Western blot analysis showed a significant 4.0 fold reduction in the protein expression of VE-cadherin in infected hBMECs in comparison with control hBMECs (Fig. 13, panel c).

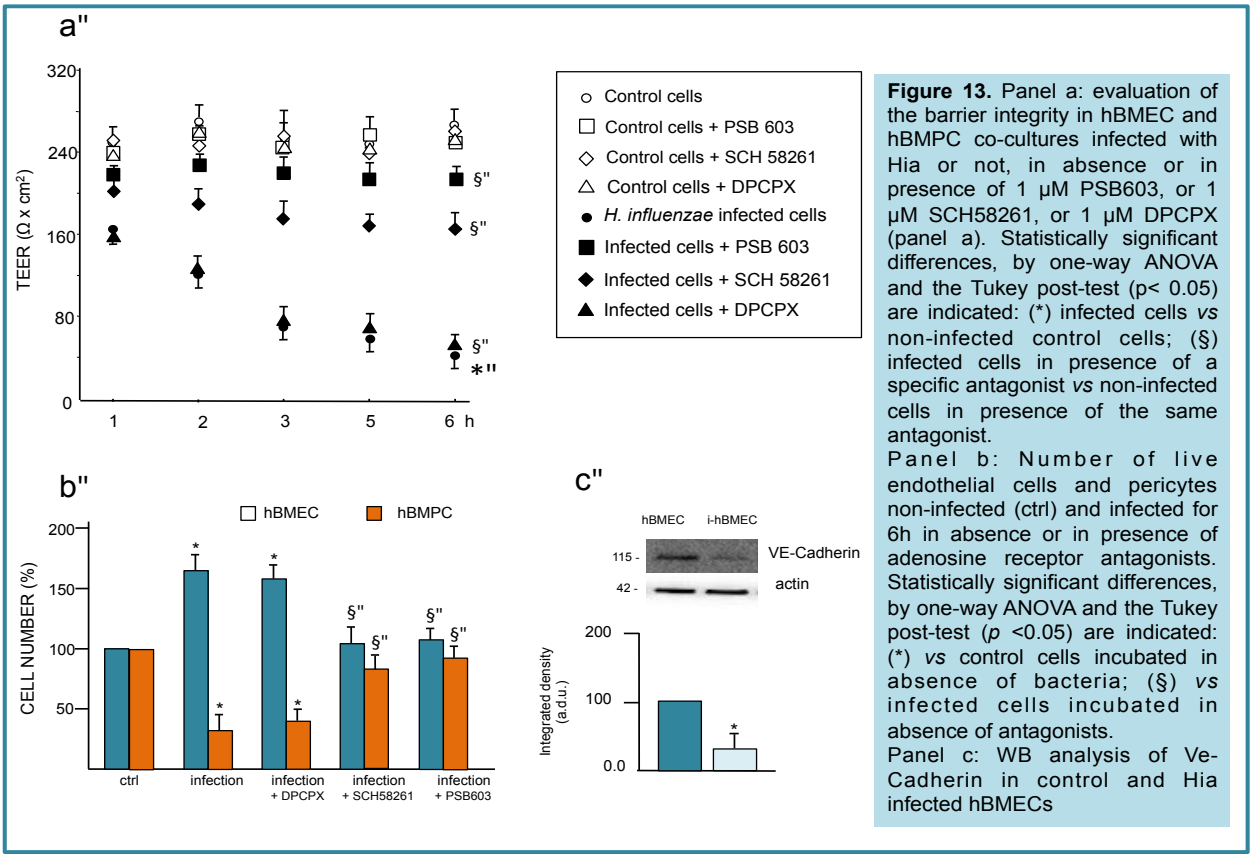

Figure 13. Panel a: evaluation of the barrier integrity in hBMEC and hBMPC co-cultures infected with Hia or not, in absence or in presence of 1 μM PSB603, or 1 μM SCH58261, or 1 μM DPCPX (panel a). Statistically significant differences, by one-way ANOVA and the Tukey post-test ($p < 0.05$) are indicated: (*) infected cells *vs* non-infected control cells; (§) infected cells in presence of a specific antagonist *vs* non-infected cells in presence of the same antagonist.
Panel b: Number of live endothelial cells and pericytes non-infected (ctrl) and infected for 6h in absence or in presence of adenosine receptor antagonists. Statistically significant differences, by one-way ANOVA and the Tukey post-test ($p < 0.05$) are indicated: (*) *vs* control cells incubated in absence of bacteria; (§) *vs* infected cells incubated in absence of antagonists.
Panel c: WB analysis of Ve-Cadherin in control and Hia infected hBMECs

We investigated the role of the different ARs on integrity of BBB by incubating the co-culture with different adenosine receptor agonists, without bacterial infection. As shown in Fig. 14, treatment of co-culture for 6h with CCPA, a specific A_1 adenosine receptor agonist, did not changed TEER values, whit respect to control cells. Co-cultures incubated with CGS 21680, a specific A_{2A}

adenosine receptor agonist, or with NECA, a generic A_2 adenosine receptor agonist, showed a decrease of TEER values by 4.3- and 3.2 fold, respectively, in comparison with control cells. Thus, we could speculate that ARs may be able to control the integrity of BBB when stinulated with physiological adenosine concentrations. Conversely, high adenosine concentrations, released after a bacterial infection (in this experiments mimed by 6h treatment with adenosine A_2 receptor agonists), could lead to breakdown of the BBB.

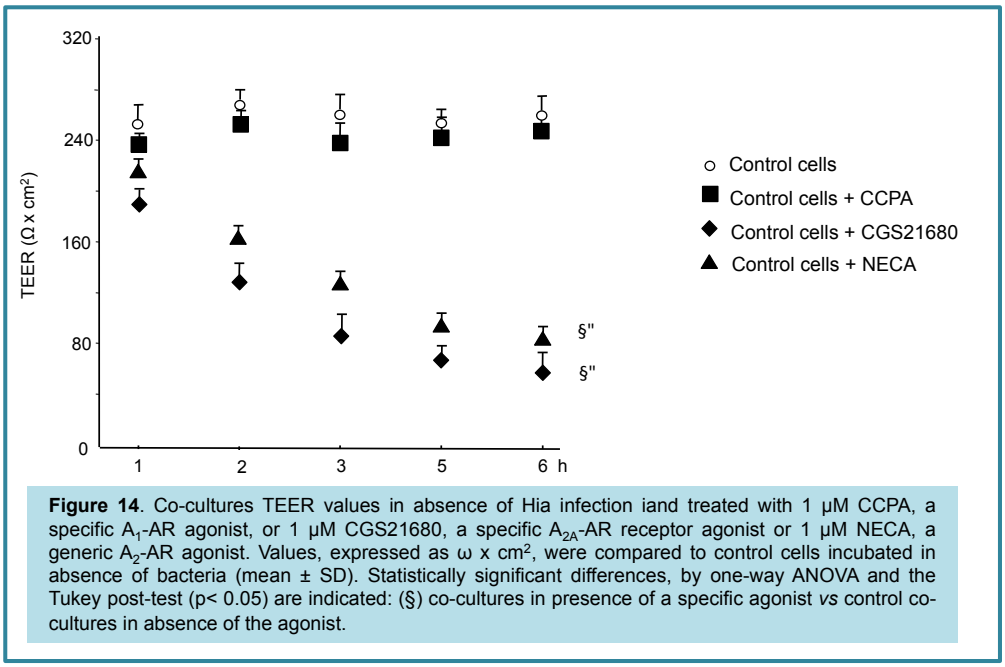

Figure 14. Co-cultures TEER values in absence of Hia infection iand treated with 1 μM CCPA, a specific A_1-AR agonist, or 1 μM CGS21680, a specific A_{2A}-AR receptor agonist or 1 μM NECA, a generic A_2-AR agonist. Values, expressed as ω x cm^2, were compared to control cells incubated in absence of bacteria (mean ± SD). Statistically significant differences, by one-way ANOVA and the Tukey post-test ($p< 0.05$) are indicated: (§) co-cultures in presence of a specific agonist *vs* control co-cultures in absence of the agonist.

Ectoenzyme activity

Ectoenzyme activity, determined by measuring Pi generated during ectoenzyme-mediated nucleotide dephosphorylation in hBMEC and hBMPC grown in mono- and in coculture, is shown in Fig. 18. After bacterial infection for 3 and 6h, the activity in hBMEC was significantly enhanced by 6.5 and 9.5 fold, respectively, indicating that bacterial infection was able to trigger adhenosine synthesis. ENTPDase activity in infected endothelial cells significantly decreased in presence of 200 □ M ARL67156, a CD39-specific inhibitor, or 100 □ M methylene adenosine-5′-diphosphate (APCP), a CD73-specific inhibitor. In particular, ectoenzyme activity decreased 3.2 and 2.9 fold,

after bacterial infection for 3h, in presence of ARL67156 and APCP, respectively and, after 6h infection, the activity decreased 4.5 and 3.8 fold in presence of ARL67156 and APCP, respectively, compared to the activity in infected cells in absence of antagonists, at the same time of incubation. No difference was found in the enzyme activity after infection of hBMPC for 3 and 6h. The concentration of Pi released in the medium of infected co-cultures increase 4.8 and 5.6 fold after infection for 3h and 6h, respectively. Ectoenzyme activity decreased 3.7 and 3.0 fold, after bacterial infection for 3h, in presence of ARL67156 and APCP, respectively and, after 6h infection, the activity decreased 3.4 and 4.2 fold in presence of ARL67156 and APCP, respectively, compared to the activity in infected cells in absence of antagonists, at the same time of incubation. The data demonstrated that in hBMEC, bacterial infection significantly activates CD39 and CD7, enzymes which determine an increase in concentration of adenosine.

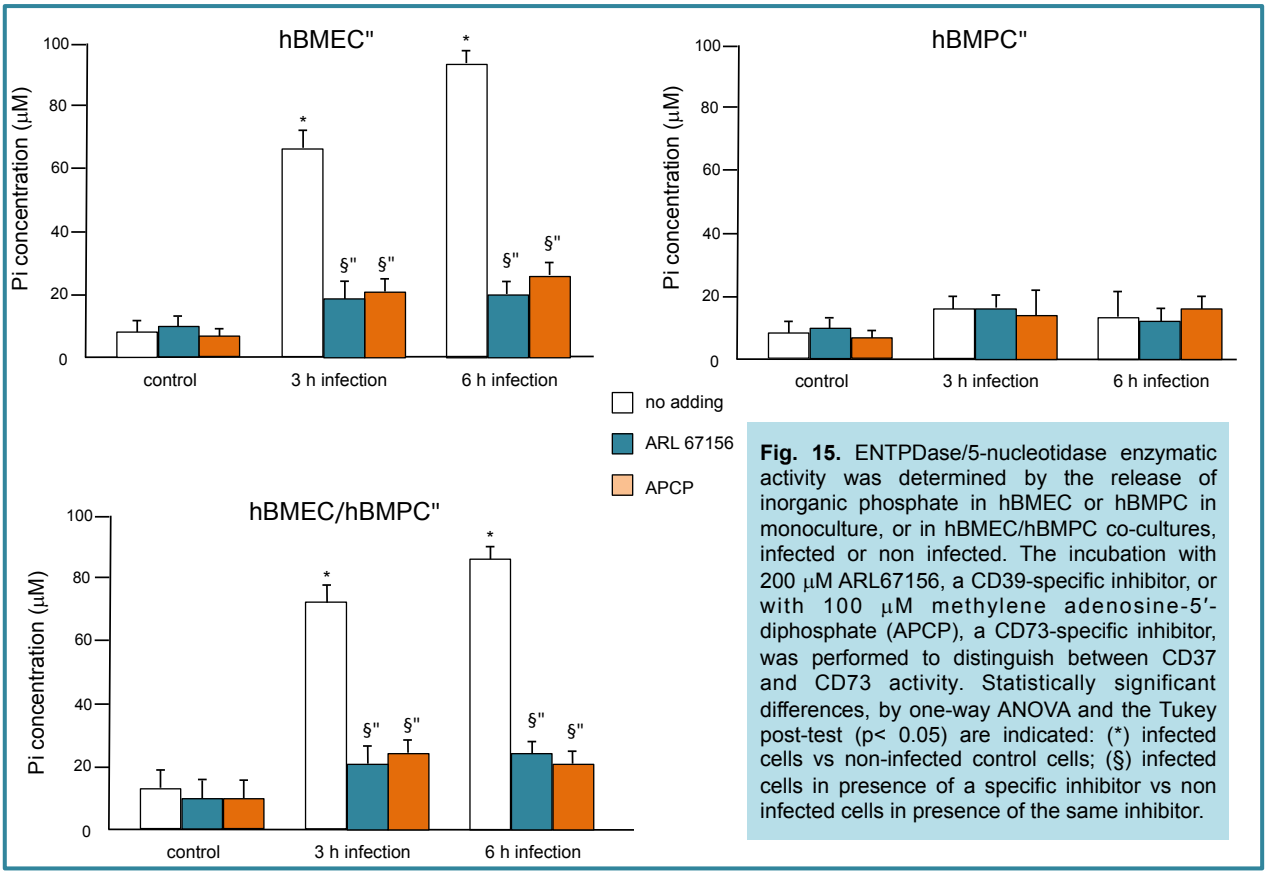

Fig. 15. ENTPDase/5-nucleotidase enzymatic activity was determined by the release of inorganic phosphate in hBMEC or hBMPC in monoculture, or in hBMEC/hBMPC co-cultures, infected or non infected. The incubation with 200 µM ARL67156, a CD39-specific inhibitor, or with 100 µM methylene adenosine-5′-diphosphate (APCP), a CD73-specific inhibitor, was performed to distinguish between CD37 and CD73 activity. Statistically significant differences, by one-way ANOVA and the Tukey post-test ($p < 0.05$) are indicated: (*) infected cells vs non-infected control cells; (§) infected cells in presence of a specific inhibitor vs non infected cells in presence of the same inhibitor.

Bacterial infection increased cAMP production in co-cultures

Fig. 16 shows cAMP levels of hBMECs and hBMPCs, grown in mono- or in co-culture, after 6h infection with Hia in absence or in presence of specific ARs antagonists. Incubation with 10 μmol/L forskolin (direct activator of adenylyl cyclase) significantly increased the amount of cAMP; similarly, 6h Hia infection significantly enhanced the production of cAMP in hBMEC mono-cultures (2.6 fold increase) in comparison with non-infected cells in absence of antagonists (Fig. 16, panel a). Infection performed in presence of SCH58261 or PSB603, decreased cAMP levels values very similar to non-infected cells without antagonists. In hBMPC monocultures (Fig. 16, panel b), forskolin significantly increased cAMP levels whilenthe infection for 6h did not changed cAMP levels, either in absence or in presence of SCH58261 or PSB603. In hBMECs grown in co-cultures, forskolin significantly increased cAMP levels (3.0 fold) with respect to non-infected cells (Fig. 16, panel c). Co-incubation of Hia with SCH58261 or PSB603, decreased cAMP levels by 2.3 fold and 2.7 fold, compared to infected cells without antagonists. Surprisingly, in hBMPCs grown in contact with hBMECs (Fig. 16, panel d), 6h infection induced an increase of cAMP very similar to forskolin treatment. Co-incubation of Hia with SCH58261 or PSB603, ecreased cAMP levels to values similar to non-infected cells. These results suggest that the response of pericytes to bacterial infection is not due to contact with bacteria but depends of release of adenosine by endothelial cells, which are very close to pericytes. Activation of adenosine A_{2A} and A_{2B} receptors results in increased cAMP levels, activation of cytosolic proteins, physiologically involved in maintaining the contractile tone, leading to detachment of pericytes from endothelial cells.

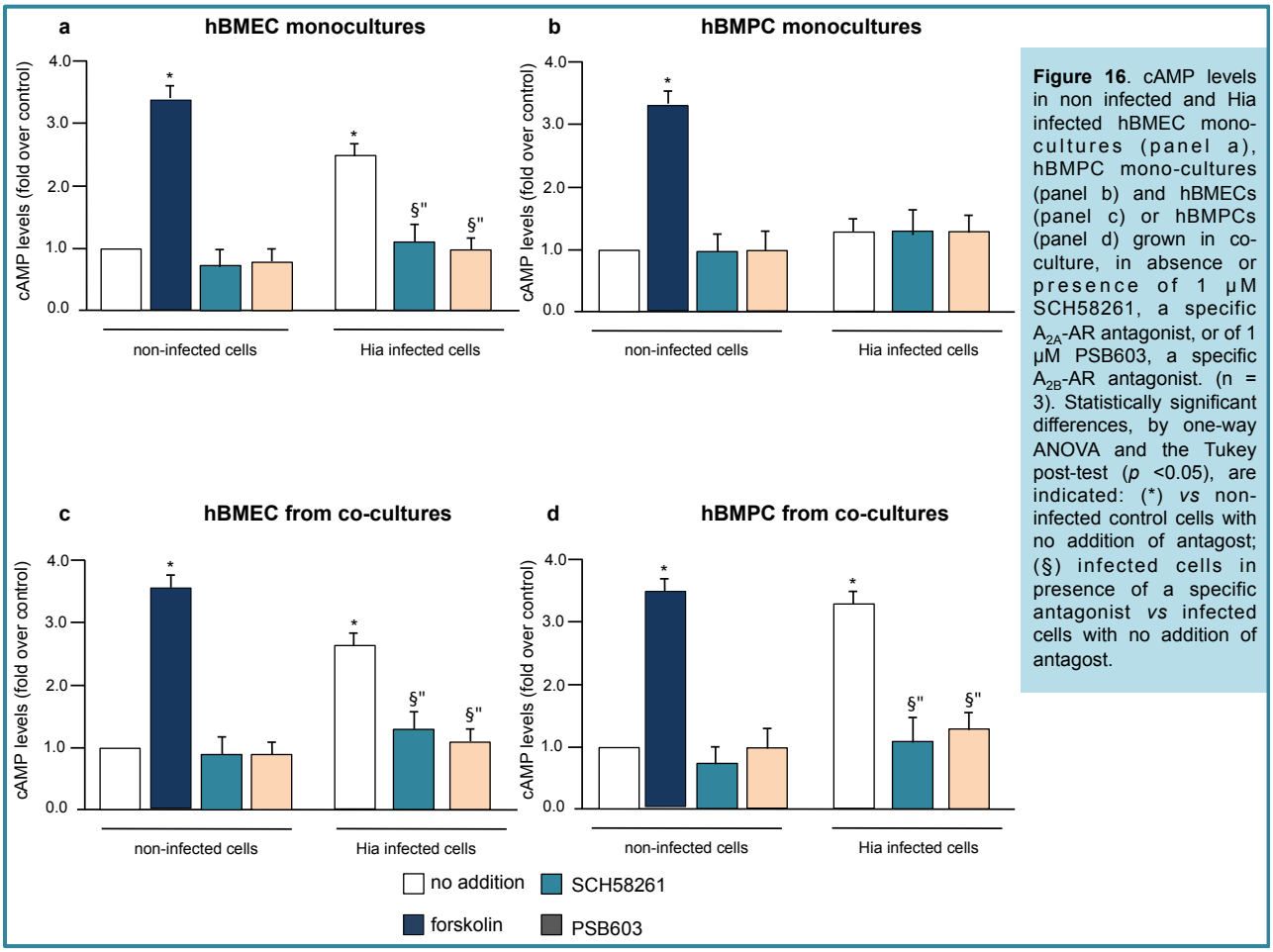

Figure 16. cAMP levels in non infected and Hia infected hBMEC mono-cultures (panel a), hBMPC mono-cultures (panel b) and hBMECs (panel c) or hBMPCs (panel d) grown in co-culture, in absence or presence of 1 μM SCH58261, a specific A_{2A}-AR antagonist, or of 1 μM PSB603, a specific A_{2B}-AR antagonist. (n = 3). Statistically significant differences, by one-way ANOVA and the Tukey post-test (p <0.05), are indicated: (*) *vs* non-infected control cells with no addition of antagost; (§) infected cells in presence of a specific antagonist *vs* infected cells with no addition of antagost.

H. influenzae stimulated VEGF release

As shown in Table 6, hBMEC-infected monoculture released 2.5 fold increase more VEGF with respect to non-infected cells; co-incubation of hBMECs in monoculture in presence of Hia and 1 μM PSB603 or 1 μM SCH58261 reduced VEGF release by 2.7- and 2.3, fold respectively, while the presence of 1 μM DPCPX during the infection did not changed VEGF release compared to infected cells in absence of antagonists.

Furthermore, VEGF released by infected co-cultures increased 2.8 fold compared to non-infected cells.The presence of PSB603 or SCH58261, but not the presence of DPCPX, reduced bacterial-induced VEGF release by 4.3- and 3.3 fold, respectively, with respect to infected co-cultures without antagonists. Moreover, treatment of non-infected co-cultures with PSB603 or SCH58261, but not with DPCPX, reduced VEGF release by 1.4- and 1.6 fold, respectively, with respect to non-

infected co-cultures without antagonists. These results suggest that the adenosine binding to its receptors, mainly A_{2A}- and A_{2B}-AR, is involved in VEGF release both during the physiological cross talk between endothelial cells and pericytes and during bacterial infection.

VEGFA (pg ml^{-1})	Control cells	Cells + *H. influenzae*
hBMEC	33.7 ± 2.1	84.5 ± 7.3**
hBMEC+PSB603	29.2 ± 2.3*	30.5 ± 2.5*
hBMEC+SCH58261	34.1 ± 2.8*	36.9 ± 3.1*
hBMEC+DPCPX	28.6 ± 2.3*	77.5 ± 6.4*
hBMPC	50.9 ± 4.8**	55.6 ± 4.4
hBMPC+PSB603	48.7 ± 3.9*	53.8 ± 5.6*
hBMPC+SCH58261	47.3 ± 4.2*	44.0 ± 3.8*
hBMPC+DPCPX	51.2 ± 4.9*	57.2 ± 4.7*
hBMEC/hBMPC	157.3 ± 11.6§	439.9 ± 38.5***
hBMEC/hBMPC+PSB603	108.6 ± 9.7*	100.5 ± 11.4*
hBMEC/hBMPC+SCH58261	97.9 ± 8.6*	131.3 ± 12.5*
hBMEC/hBMPC+DPCPX	148.8 ± 10.1*	446.3 ± 40.8*

Table 6. VEGFA determination in hBMECs and hBMPCs in mono- and co-culture infected and non-infected by *H. influenzae*. Cell culture supernatants from mono- and co-cultures in absence (control) and presence of *H. influenzae* (10^7 CFU/well), for 6h, with or w/o 1 μM PSB603, a specific A_{2B} adenosine receptor antagonist or with 1 μM SCH58261, a specific A_{2A} adenosine receptor antagonist or with 1 μM DPCPX, a specific A_1 adenosine receptor antagonist, were assayed for VEGF release. Inhibitors were added to the culture medium 60 min before *H. influenzae* addition.
Values (means ± S.E.M.) are from three independent experiments (n = 3). Statistically significant differences by one-way ANOVA and the Tukey *post-test* ($p<0.05$) are indicated. (*) *vs* the same group w/o inhibitors; (**) *vs* control hBMEC; (***) *vs* control hBMEC / hBMPC co-cultures; (§) $p<0.05$ *vs* mono-cultures.

To deeper demonstrate the involvement of VEGF in BBB impairment generated by Hia infection, TEER analysis was performed in presence of specific antibodies blocking VEGF-R1 or VEGF-R2 (Fig. 17). Hia reduced TEER values, which were rescued by co-incubation with VEGF-R1 and VEGF-R2 Abs, thus demonstrating that VEGF, released after Hia infection, may be responsible for the endothelial cell proliferation and consequent BBB collapse.

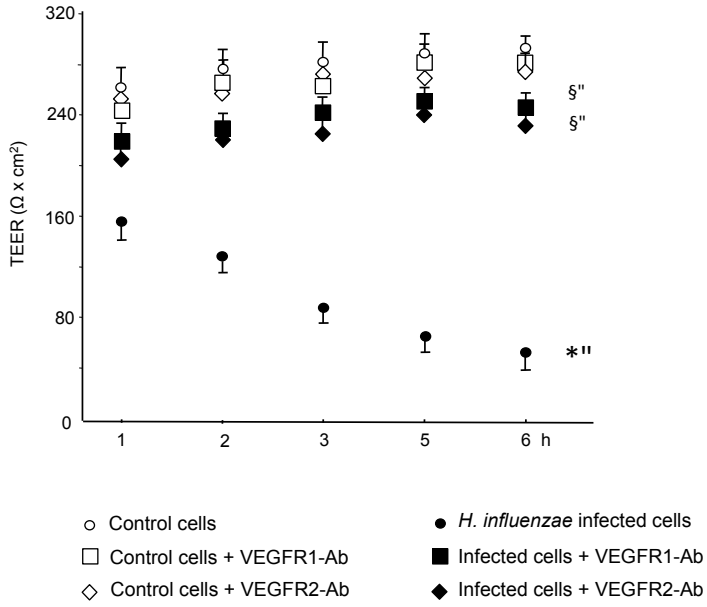

Figure 17. TEER values of co-culture, non infected and Hia infected, in presence of specific antibodies able to block VEGF-R1 or VEGF-R2. Values, expressed as ω x cm^2, were compared to control cells incubated in absence of bacteria (mean ± SD) and were from three independent experiments (n = 3). Statistically significant differences, by one-way ANOVA and the Tukey post-test ($p < 0.05$) are indicated: (*) *vs* control cells incubated in absence of bacteria; (§) *vs* co-cultures in absence of VEGF-R1/2 antibodies.

CREB and Rho activation in co-cultures

It is known that the transcription factor CREB is involved in the expression of VEGF in microvascular endothelial cells after A_{2B}-AR stimulation (Acurio *et al*., 2016; Du *et al.*, 2015). It is also known that Rho mediates BBB permeability by inducing morphological changes in actin-cytoskeletal reorganization (Do-Geun *et al.*, 2015). For these reason, we decided to address the effects of A_{2A} and A_{2B}-AR antagonists on CREB and Rho activation in hBMECs/hBMPCs co-culture after Hia infection. CREB and Rho-A protein expression did not changed in control and infected hBMECs in absence or in presence of antagonists. Phosphorylation of CREB and Rho-A significantly increased after Hia infection of hBMECs, with respect to non-infected cells, and the co-incubation with SCH58261 and PSB603 significantly abrogated the phosphorylation of CREB and Rho-A induced by infection (Fig. 18). Likewise, CREB and Rho-A protein expression did not changed in control and infected hBMPCs, in absence or in presence of antagonists. Phosphorylation of CREB and Rho-A significantly increased in infected hBMPC and was significantly reduced in response to A_{2A}- and A_{2B}-ARs antagonists (Fig. 19).

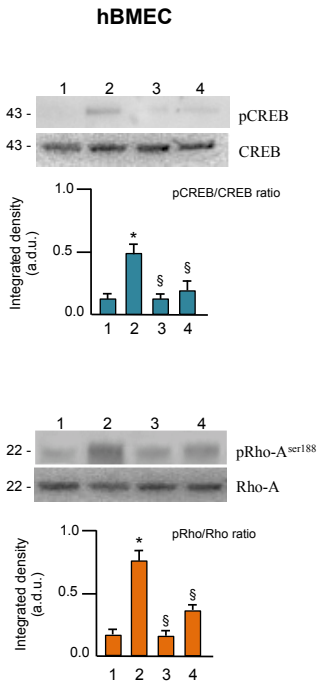

1. Control cells
2. Infected cells
3. Infected cells + SCH58261
4. Infected cells + PSB603

Figure 18. Expression of CREB, p-CREB, Rho-A and p-Rho-A evaluated by Western blot analyses in control and Hia infected hBMECs grown in co-culture with hBMPCs in presence of 1 μM of SCH58261 or 1 μM PSB603. Statistically significant differences, determined by one-way ANOVA and the Tukey post-test (p <0.05), are indicated: (*) infected cells *vs* non-infected control cells; (§) infected cells in presence of a specific antagonist *vs* infected cells in absence of antagonist.

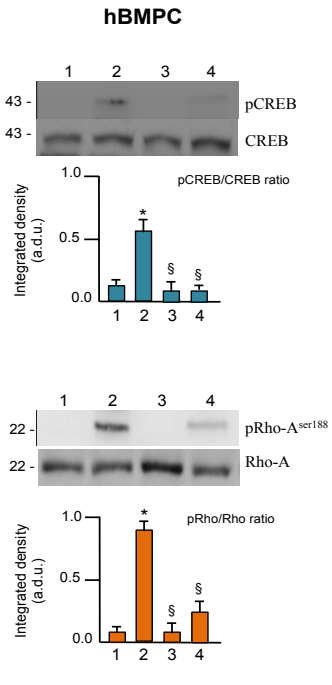

1. Control cells
2. Infected cells
3. Infected cells + SCH58261
4. Infected cells + PSB603

Figure 19. Expression of CREB, p-CREB, Rho-A and p-Rho-A evaluated by Western blot analyses in control Hia infected hBMPCs grown in co-culture with hBMECs in presence of 1 μM of SCH58261 or 1 μM PSB603. Statistically significant differences, determined by one-way ANOVA and the Tukey post-test (p <0.05), are indicated: (*) infected cells *vs* non-infected control cells; (§) infected cells in presence of a specific antagonist *vs* infected cells in absence of antagonist.

DISCUSSION

This study highlights the role of A_2A and A_2B adenosine receptors in maintaining the integrity of the blood brain barrier following Hia infection. The peculiar characteristic of endothelial cells of the brain microvessels is to possess TJs at their intercellular contacts (Wolburg et al., 2002; Weksler et al., 2005), responsible for their ability to block the passage of many agents. The in vitro model of BBB, used in this study and characterized by high TEER values, was performed by co-culturing human brain microvascular endothelial cells and pericytes; in these conditions, the two cell types have reproduced the physiological conditions present in BBB, thus repeating the highly effective barrier that separates the brain micro-environment from the circulating blood.

The interaction between the pathogenic microorganisms and the microvascular endothelial cells, responsible of the crossing of BBB, is characterized by several steps, the first of which is the link between host receptors and bacterial components (St Geme et al., 1996). Hia can interact with microvascular endothelial cells via OmpP2, which binds to the carboxy-terminal domains of laminin receptors (Orihuela et al., 2009) or by using pili or fibrils (St Geme et al., 1996). An important role, during the early phases of Hia adhesion, plays the platelet activating factor receptors, which facilitates the cross of bacteria into the CNS (Swords et al., 2001). The adhesion to these internalization receptors allows Hia to enter microvascular endothelial cells, thus determining the BBB collapse.

It has been shown that the breakdown of the barrier can be caused both by intracellular crossing of bacteria and their paracellular translocation; this latter mechanism is used by bacteria belonging to the Haemophylus family, which can cross the BBB and colonize the brain from the respiratory tract of infected patients (Dando et al., 2014).

In this study, we demonstrated that Hia cross the BBB with either intracellular and paracellular mechanism, as evidenced by TEM images. After contact between Hia and co-cultures

of endothelial cells and pericytes for 6h, the bacteria are visible both into endothelial cells and between the cells, demonstrating that both mechanisms are used by Hia to reach the brain .

Data obtained from invasion assays showed that a high percentage of bacteria were localized within the endothelial cells after 6h, and the confirmation of this result was provided by SEM and TEM images. At the same time of incubation, the cell count highlighted a reduction in the pericyte number and an increase in the endothelial cells number. The increased endothelial proliferation confirms the data from literature demonstrating the role of pericytes in the control of endothelial proliferation and in the stabilization of the microvessels (Trost et al., 2016). The consequence of this series of events is the BBB collapse, highlighted by a sharp reduction in both TEER values and VE-cadherin expression after infection by Hia for 6h.

Many factors, such as transforming growth factor β, angiopoietins, platelet-derived growth factor β, spingosine-1-phosphate and Notch have a pivotal role in the intercellular communication between endothelial cells and pericytes (Dore-Duffy, 2008). It has been demonstrated the significant role of adenosine receptors in the maintaining of BBB permeability (Bynoe et al., 2015) and the presence of CD73 ecto-enzymes in hBMECs as well as the involvement of AR signaling in the modulation of BBB permeability following the binding of selective agonists (Do-Geun et al., 2015), thus promoting the entry of macromolecules into the CNS. Conversely, the reduction of the passage of macromolecules into the brain by AR antagonists makes the binding of the adenosine to a specific receptor in the BBB as a key that allows or blocks the passage of substances and bacteria by (Bynoe et al., 2015).

We speculated that the infection of brain endothelial cells can cause production of high concentration of adenosine which in turn could activate AR of adjacent pericytes, increasing BBB permeability. It has been demonstrated that the activation of A_{2A} AR causes relaxation of pericytes (Matsugi et al., 1997) and that the activation of AR in pericytes determines the opening of the K^+-ATP channel and the increase of the capillary blood flow (Li et al., 2001).

By measuring the inorganic phosphate (Pi) generated during the ectoenzyme-mediated

nucleotide dephosphorylation in hBMEC grown in mono-culture and in hBMEC/hBMPC coculture, we indirectly demonstrated, that bacterial infection significantly activates CD39 and CD73 enzymes (ecto-enzymes responsible for generating extracellular adenosine), determining an increase in adenosine concentration. Differently, in hBMPC in mono-culture, the infection did not activate the ecto-enzymes. It has been already demonstrated that CD39 and CD73 are highly expressed on both primary human brain endothelial cells and human brain endothelial cell line HCMEC-D3 and that A_{2A} AR activation increases paracellular permeability in primary human brain endothelial cell monolayers (Do-Geun *et al.*, 2015).

Experiments, performed by infecting co-cultures in the presence of different AR antagonists demonstrated that the inhibition of A_{2A} and A_{2B} AR, but not A_1 AR, maintains unaltered the barrier characteristics. This was evidenced by high TEER values when infection by Hia was conducted in the presence of PSB 603, a specific A_{2B} adenosine receptor antagonist or with SCH58261, a specific A_{2A} adenosine receptor antagonist but not in the presence of DPCPX, a specific A_1 adenosine receptor antagonist. These results confirmed that A_1AR does not seem to be involved in BBB disfunction following Hia infection. Furthermore, PSB 603 and SCH58261 were able to prevent the pericytes loss following bacterial infection and consequently to prevent endothelial cells uncontrolled proliferation. In contrast, in the presence of DPCPX, the pericyte number remained very low after bacterial infection.

These results agree with those of other studies demonstrating that functional A_2 ARs are present on hBMPCs and hBMECs while the A_1 subclass is relatively inactive biologically, and highlighting the importance of cross-talk between the two cellular components in the maintaining of the integrity of the BBB (Takagi et al., 1996).

To further confirm data obtained, experiments were conducted by incubating non-infected cells with AR agonists: TEER values were significantly reduced when co-cultures were incubated with CGS 21680, a specific A_{2A} adenosine receptor agonist, or with NECA, a generic A_2 adenosine receptor agonist, highlighting the role of A_{2A} and A_{2B} AR in maintaining the BBB characteristics.

Furthermore, in hBMECs, both in mono- and in co-culture, the cAMP levels were found high after Hia infection, confirming that A_2 AR was stimulated by Hia infection but not A_1 AR, because its stimulation does not increase cAMP levels. Furthermore, after infection for 6h, pericytes in co-culture with endothelial cells, but not pericytes in mono-culture, produced high cAMP concentrations, confirming that adenosine produced by endothelial cells can bind AR on pericytes.
In infected hBMECs, both in mono- and in co-culture, and in hBMPCs in co-culture, cAMP concentration was reduced in the presence of A_{2A} and A_{2B} AR antagonists. This data suggests that hBMECs produced high adenosine concentrations after bacterial infection and that adenosine binds AR on pericytes, determining their detachment.

Our results also demonstrated that bacterial infection promotes the VEGF release in hBMPCs in co-culture and in hBMECs, both in mono- and in co-culture. Adenosine could be an important putative messenger responsible for the VEGF release by binding AR on endothelial cells. VEGF could be responsible for the BBB impairment after bacterial infection, because the blocking of VEGF receptors shields the BBB from the infection-induced breakdown (Anfuso et al., 2014; Lupo et al., 2014). These results were confirmed by data demonstrating that A_{2B} AR activation is involved in the induction of angiogenesis and VEGF production from BMECs and that A_{2A} AR stimulates VEGF gene expression in response to hypoxia-induced accumulation of adenosine in retinal vascular cells (Ryzhov et al., 2014).

In the model of BBB used in our experiments, we demonstrated that bacterial infection induced the activation of CREB and Rho-A and that A_{2A} and A_{2B} antagonists were able to inactivate them. Previous studies demonstrated the up-regulation of VEGF and cAMP-PKA-CREB signaling pathway in adenosine-induced angiogenesis in human endothelial cells (Yang et al., 2016; Nathan et al., 2016) and an A_{2A}-induced increase in Rho-A activity, cytoskeletal modification and BBB permeability (Do-Geun et al., 2015).

Our study, according to recent reports in literature, demonstrated that the moderate increase in adenosine concentration is able to inducing beneficial effects such as vasodilation and control of

the release of inflammatory molecules; chronic overproduction of adenosine, which can occur during various pathologies (Borea et al., 2017), can have adverse effects on the functionality of different organs and on BBB, which can undergo to the loss of its features. Among the pathologies involved in the over-production of adenosine, the bacterial infection also plays an important role. Bacterial meningitis is an important cause of child mortality in the clinical setting (Almeida et al., 2017; Hammitt et al., 2005; Ouchenir et al., 2017), and this study demonstrated the correlation between the signalling pathway, triggered by adenosine, and BBB breakdown after Hia infection, highlighting the modulatory role of A_{2A} and A_{2B} adenosine receptors.

The innovative aspect of this research is based on the demonstration of the existence of adenosine signalling in microvascular pericytes, responsible for TJ formation between endothelial cells and for the control of endothelial proliferation, thus inducing BBB properties. To date, the involvement of pericital adenosine receptors in Hia infection response has not been demonstrated.

Because the pericytes play a crucial role in microvascular stabilization, the reduction of the pericyte number during bacterial meningitis is a particularly important event responsible for the loss of the barrier functions. For their function, pericytes could be highly suitable for cell-based therapies in many infectious diseases, and the study of pathways leading to pericyte malfunction throws the bases for the development of new pharmaceutical targets.

Reference list, second study

Abbott NJ, Patabendige AA, Dolman DE, Yusof SR, Begley DJ (2010) Structure and function of the blood-brain barrier. Neurobiol Dis 37:13–25.

Acurio J, Herlitz K, Troncoso F, Aguayo C, Bertoglia P, Escudero C (2016) Adenosine A2A receptor regulates expression of vascular endothelial growth factor in feto-placental endothelium from normal and late-onset pre-eclamptic pregnancies. Purinergic Signal 13(1):51-60. doi: 10.1007/s11302-016-9538-z.

Almeida AF, Trindade E, B Vitor A, Tavares M (2017) Haemophilus influenzae type b meningitis in a vaccinated and immunocompetent child. J Infect Public Health 10(3):339-342. doi: 10.1016/j.jiph.2016.06.001.

Anfuso CD, Motta C, Giurdanella G, Arena V, Alberghina M, Lupo G (2014) Endothelial PKCa / MAPK/ERK-phospholipase A2 pathway activation as a response of glioma in a triple culture model. A new role for pericytes? Biochimie 99:77-87.

Borea PA, Gessi S, Merighi S, Vincenzi F, Varani K (2017) Pathologic overproduction: the bad side of adenosine. Br J Pharmacol. doi: 10.1111/bph.13763.

Bynoe MS, Viret C, Yan A, Kim DG. (2015) Adenosine receptor signaling: a key to opening the blood-brain door. Fluids Barriers CNS 12:20. doi 10.1186/s12987-015-0017-7.

Carman AJ, Mills JH, Krenz A, Kim DG, Bynoe MS (2011) Adenosine receptor signaling modulates permeability of the blood-brain barrier. J Neurosci 31(37):13272–80.

Dando SJ, Mackay-Sim A, Norton R et al (2014) Pathogens Penetrating the Central Nervous System: Infection Pathways and the Cellular and Molecular Mechanisms of Invasion. Clin Microbiol Rev 27(4):691. doi: 10.1128/CMR.00118-13.

Dejana E, Tournier-Lasserve E, Weinstein BM (2009) The control of vascular integrity by endothelial cell junctions: molecular basis and pathological implications. Dev Cell 16:209–221.

Denk-Lobnig M, Martin AC (2017) Modular regulation of Rho family GTPases in development. Small GTPases 17:1-8.

Dore-Duffy P (2008) Pericytes: pluripotent cells of the blood brain barrier. Curr Pharm Des 14:1581–1593.

Do-Geun K and Bynoe MS (2015) A2A adenosine receptor regulates the human blood brain barrier permeability. Mol Neurobiol 52(1): 664–678.

Du X, Ou X, Song T, Zhang W, Cong F, Zhang S, Xiong Y (2015) Adenosine A2B receptor stimulates angiogenesis by inducing VEGF and eNOS in human microvascular endothelial cells. Exp Biol Med 240(11):1472-9.

Gona F, Barbera F, Pasquariello AC et al (2014) In vivo multiclonal transfer of bla(KPC-3) from Klebsiella pneumoniae to Escherichia coli in surgery patients. Clin Microbiol Infect 20(10):633-5.

Hammitt LL, Block S, Hennessy TW, Debyle C, Peters H, Parkinson A, et al (2005) Outbreak of invasive Haemophilus influenzae serotype a disease. Pediatr Infect Dis J 4:453–6.

Jin Z, Romero-Steiner S, Carlone GM, Robbins JB, Schneerson R (2007) Haemophilus influenzae type a infection and its prevention. Infect Immun 75:2650–4.

Kim KS (2003) Pathogenesis of bacterial meningitis: from bacteraemia to neuronal injury. Nat Rev Neurosci 4:376–385.

Kim KS (2008) Mechanisms of microbial traversal of the blood- brain barrier. Nat Rev Microbiol 6:625–634.

Ladhani S, Slack MP, Heath PT, von Gottberg A, Chandra M, Ramsay ME (2010) Invasive Haemophilus influenzae disease, Europe, 1996–2006. Emerging Infectious Diseases 16(3) 455–463.

Li Q, and Puro DG (2001) Adenosine activates ATP-sensitive K□ currents in pericytes of rat retinal microvessels: role of A1 and A2a receptors. Brain Res 907:93–99.

Lima JBT, Ribeiro GS, Cordeiro SM et al (2010) Poor clinical outcome for meningitis caused by Haemophilus influenzae serotype A strains containing the IS1016-bexA deletion. Journal of Infectious Diseases 202(10):1577–1584.

Lupo G, Motta C, Salmeri M, Spina-Purrello V, Alberghina M, Anfuso CD (2014) An in vitro retinoblastoma human triple culture model of angiogenesis: A modulatory effect of TGF-β. Cancer Letters 354:181–188.

Matsugi T, Chen Q, Anderson DR (1997) Adenosine-induced relaxation of cultured bovine retinal pericytes. Invest Ophthalmol Vis Sci 38(13):2695-701.

Motta C, Salmeri M, Anfuso CD et al (2014) Klebsiella pneumoniae induces an inflammatory response in an in vitro model of blood-retinal barrier. Infect Immun 82(2):851-63.

Nathan JR, Lakshmanan G, Michael FM, Seppan P, Ragunathan M (2016) Expression of adenosine receptors and vegf during angiogenesis and its inhibition by pentoxifylline-A study using zebrafish model. Biomed Pharmacother 84:1406-1418.

Orihuela CJ, Mahdavi J, Thornton J et al (2009) Laminin receptor initiates bacterial contact with the blood brain barrier in experimental meningitis models. J Clin Invest 119(6):1638–1646.

Ouchenir L, Renaud C, Khan S, et al (2017) The Epidemiology, Management, and Outcomes of Bacterial Meningitis in Infants. Pediatrics e20170476. doi: 10.1542/peds.2017-0476.

Pettengill MA, Lam VW, Ojcius DM (2009) The danger signal adenosine induces persistence of chlamydial infection through stimulation of A2b receptors. PLoS One 14(12):e8299.

Prajapati K, Raj S, Mullan S. (2017) Different Preservation Methods for Long Term Maintenance of Haemophilus influenzae. Advances in Microbiology 7:343-348.

Ryzhov S, Biktasova A, Goldstein AE, Zhang Q, Biaggioni I, Dikov MM, Feoktistov I (2014) Role of JunB in adenosine A2B receptor-mediated vascular endothelial growth factor production. Mol Pharmacol 85:62–73.

Salmeri M, Motta C, Anfuso CD et al (2013) VEGF receptor-1 involvement in pericyte loss induced by Escherichia coli in an in vitro model of blood brain barrier. Cell Microbiol 15(8):1367-84. doi:10.1111/cmi.12121.

Slack MPE (2006) Haemophilus. 10th edition In: Borriello SP, Murray PR, Funke G (ed) Topley & Wilson's microbiology and microbial infections, 2. London, UK: Edward Arnold Ltd 1692–718.

Souza LF, Jardim FR, Sauter IP, Souza MM, Barreto F, Margis R, Bernard EA (2009) Lipoteichoic acid from Staphylococcus aureus increases matrix metalloproteinase 9 expression in RAW 264.7 macrophages: modulation by A2A and A2B adenosine receptors. Mol Immunol 46(5):937-42.

St Geme JW 3rd, Cutter D (1996) Influence of pili, fibrils, and capsule on in vitro adherence by Haemophilus influenzae type b. Mol Microbiol 21(1):21–31.

Stefani S, Mezzatesta ML, Fadda G et al (2008) Antibacterial activity of cefditoren against major community-acquired respiratory pathogens recently isolated in Italy. J Chemother 20(5):561-9.

Swords WE, Ketterer MR, Shao J, Campbell CA, Weiser JN, Apicella MA (2001) Binding of the non- typeable Haemophilus influenzae lipooligosaccharide to the PAF receptor initiates host cell signalling. Cell Microbiol 3(8):525–536.

Takagi H, King GL, Robinson GS, Ferrara N, Aiello LP (1996) Adenosine Mediates Hypoxic Induction of Vascular Endothelial Growth Factor in Retinal Pericytes and Endothelial Cells. Investigative Ophthalmology & Visual Science 37(11):2165-76.

Trost A, Lange S, Schroedl F et al (2016) Brain and Retinal Pericytes: Origin, Function and Role. Front Cell Neurosci 10:20. doi: 10.3389/fncel.2016.00020.

Ulanova M, Tsang RSW (2009) Invasive Haemophilus influenzae disease: changing epidemiology and host-parasite interactions in the 21st century. Infection, Genetics and Evolution 9(4) 594–605.

Ulanova M, Tsang RSW (2014) Haemophilus influenzae serotype a as a cause of serious invasive infections. Lancet Infect Dis 14(1):70-82.

Warren CA, Li Y, Calabrese GM, Freire RS et al (2012) Contribution of adenosine A(2B) receptors in Clostridium difficile intoxication and infection. Infect Immun 80(12):4463-73.

Weksler BB, Subileau EA, Perriere N et al (2005) Blood–brain barrier-specific properties of a human adult brain endothelial cell line. FASEB 19(13):1872–1874.

Winkler EA, Bell RD, Zlokovic BV (2011) Central nervous system pericytes in health and disease. Nat Neurosci 14: 1398–1405.

Wolburg H, Lippoldt A (2002) Tight junctions of the blood–brain barrier: development, composition and regulation. Vascul Pharmacol 38(6):323–337.
Zarei AE, Almehdar HA, Redwan EM (2016) Hib Vaccines: Past, Present, and Future Perspectives. J Immunol Res:7203587.

Yang R, Liu W, Miao L et al (2016) Induction of VEGFA and Snail-1 by meningitic Escherichia coli mediates disruption of the blood-brain barrier. Oncotarget 7(39):63839-55.

Zhu L, Maruvada R, Sapirstein A, Malik KU, Peters-Golden M, Kim KS (2010) Arachidonic acid metabolism regulates Escherichia coli penetration of the blood-brain barrier. Infect Immun 78:4302–4310.

ACKNOWLEDGEMENTS

I would like to thank all those persons that during the last three years, in various manners, have supported my work.

Prof. Mario Salmeri, who introduced me to Proff. Gabriella Lupo and C. Daniela Anfuso. They all together gave me the great opportunity to improve my personal and scientifical skills. Thanks for all the teachings, all the support and thanks for the trust you always given me.

Special thanks to Prof. Massimo Libra and Dr. Giovanni Ligresti for my amazing and exciting experience in USA.

Thanks to my lab colleagues, my special friends Melania, Martina and Giovanni for the funny moments spent together and for the encouragement when the experiments did not work.

Thanks to my fiancé Damiano, who totally supported me during my USA experience. Without him, I would not have been able to do it.

Finally, I want say thanks to my parents, for their love and support during difficult moments.

Papers published during doctorate

Caporarello N, *Olivieri M, Cristaldi M, Scalia M, Toscano MA, Genovese C, Addamo A, Salmeri M, Lupo G, Anfuso CD.* "Blood-Brain Barrier in a Haemophilus influenzae Type a In Vitro Infection: Role of Adenosine Receptors A2A and A2B". Mol Neurobiol 2017 Sep 18. doi: 10.1007/s12035-017-0769-y.

Caporarello N*, Olivieri M, Cristaldi M, RuscianoD, Lupo G, Anfuso CD*. "Melanogenesis in uveal melanoma cells: Effect of argano oil". Int J Mol Med. 2017 Oct;40(4):1277-1284. doi: 10.3892/ijmm.2017.3104.

Caporarello Nunzia*, Parrino Cristina, Trischitta Vincenzo, Frittitta Lucia.* "Insulin Receptor Signaling and Glucagon-Like Peptide 1 Effects On Pancreatic Beta cells". PLos Pne. 2017 Aug 2;12(8):e0 181190. doi: 10.1371/journal.pone.0181190. eCollection 2017.

Nunzia Caporarello*, Gabriella Lupo, Melania Olivieri, Martina Cristaldi, Maria Teresa Cambria, Mario Salmeri and Carmelina Daniela Anfuso.* "Classical VEGF, Notch and Ang signalling in cancer angiogenesis, alternative approaches and future directions". Mol Med Rep. 2017 Oct;16(4):4393-4402. 10.3892/mmr.2017.7179.

Giovanni Giurdanella, Francesca Lazzara, ***Nunzia Caporarello****, Gabriella Lupo, Carmelina Daniela Anfuso, Chiara M. Eandi, Gian Marco Leggio, Filippo Drago, Claudio Bucolo, Salvatore Salomone.* "Sulodexide prevents activation of the PLA2/COX-2/VEGF inflammatory pathway in human retinal endothelial cells by blocking the effect of AGE/RAGE". Biochem Pharmacol. 2017 Oct 15;142:145-154. doi: 10.1016/j.bcp.2017.06.130.

Lupo G, ***Caporarello N****, Olivieri M, Cristaldi M, Motta C, Bramanti V, Avola R, Salmeri M, Nicoletti F, Anfuso CD*. "Anti-angiogenic Therapy in Cancer: Downsides and New Pivots for Precision Medicine". Front Pharmacol. 2017 Jan 6;7:519. doi: 10.3389/fphar.2016.00519. Review.

Melania Olivieri, Emanuele Amata, Shila Vinciguerra, Jole Fiorito, Giovanni Giurdanella, Filippo Drago, ***Nunzia Caporarello****, Orazio Prezzavento, Emanuele Arena, Loredana Salerno, Antonio Rescifina, Gabriella Lupo, Carmelina Daniela Anfuso and Agostino Marrazzo.* "Antiangiogenic Effect of (±)-Haloperidol Metabolite II Valproate ester [(±)-MRJF22] in Human Microvascular Retinal Endothelial Cells. J Med Chem 2016, doi: 10.1021/acs.jmedchem.6b01039.IF 2016: 5.59

Daniele Tibullo, ***Nunzia Caporarello,*** *Cesarina Giallongo, Carmelina Daniela Anfuso, Claudia Genovese, Carmen Arlotta, Fabrizio Puglisi, Nunziatina L. Parrinello, Vincenzo Bramanti, Alessandra Romano, Gabriella Lupo, Valeria Toscano, Roberto Avola, Maria Violetta Brundo, Framcesco Di Raimondo, Salvatore Raccuia.* "Antiproliferative and Antiangiogenic effects of *Punica granatum* Juice (PGJ) in Multiple Myeloma (MM). Nutrients 2016, 8, 611; doi:103390/nu8100611.

Nunzia Caporarello*, Mario Salmeri, Marina Scalia, Carla Motta, Cristina Parrino, Lucia Frittitta, Melania Olivieri, Martina Cristaldi, Roberto Avola, Vincenzo Bramanti, Maria Antonietta Toscano, Carmelina Daniela Anfuso, Gabriella Lupo.* "Cytosolic and Calcium-Independent Phospholipase A_2 activation and Prostaglandin E_2 are associated eith Escherichia coli-induced reduction of insulin secretion in INS-1E cells. PLoS One. 2016, 11(9): e0159874. Epub: 2016 Sep 15.

Caporarello N, *Salmeri M, Scalia M, Motta C, Parrino C, Frittitta L, Olivieri M, Toscano M A, Anfuso C D, Lupo*. "Role of cytosolic and calcium independent phospholipases A_2 in insulin secretion impairment of INS-1E cells infected by S. aureus". FEBS Lett. 2015 Dec 21; 589 (24 Pt B): 3969-76. doi: 10.1016/j.febslet.2015.11.035. Epub 2015 Nov 26.

AnfusoC D, Olivieri M, Bellanca S, Salmeri M, Motta C, Scalia M, Satriano C, La Vignera S, Burrello N, ***Caporarello N****, Lupo G, Calogero A E*. "Asthenozoospermia and membrane remodeling enzymes: A new role for phospholipase A_2". Andrology. 2015 Nov;3(6):1173-82. doi: 10.1111/andr.12101. Epub 2015 Oct 7.

Giurdanella G, Anfuso C D, Olivieri M, Lupo G, ***Caporarello N****, Eandi C M, Drago F, Bucolo C, Salomone S* "Aflibercept, bevacizumab and ranibizumab prevent glucose-induced damage in human retinal pericytes in vitro, through a PLA_2/COX-2/ VEGF-A pathway". Biochem Pharmacol. 2015 Aug 1;96(3):278-87.